



Calhoun: The NPS Institutional Archive
DSpace Repository

Theses and Dissertations

1. Thesis and Dissertation Collection, all items

2013-06

The effects of shoaling internal tides on benthic exchange events and near-boundary mixing along the continental shelf

Pastrana, Darren L.

Monterey, California. Naval Postgraduate School

<http://hdl.handle.net/10945/34719>

This publication is a work of the U.S. Government as defined in Title 17, United States Code, Section 101. Copyright protection is not available for this work in the United States.

Downloaded from NPS Archive: Calhoun



Calhoun is the Naval Postgraduate School's public access digital repository for research materials and institutional publications created by the NPS community. Calhoun is named for Professor of Mathematics Guy K. Calhoun, NPS's first appointed -- and published -- scholarly author.

Dudley Knox Library / Naval Postgraduate School
411 Dyer Road / 1 University Circle
Monterey, California USA 93943

<http://www.nps.edu/library>



NAVAL POSTGRADUATE SCHOOL

MONTEREY, CALIFORNIA

THESIS

**THE EFFECTS OF SHOALING INTERNAL TIDES ON
BENTHIC EXCHANGE EVENTS AND NEAR-
BOUNDARY MIXING ALONG THE CONTINENTAL
SHELF**

by

Darren L. Pastrana

June 2013

Thesis Advisor:
Second Reader:

Timothy Stanton
William Shaw

Approved for public release; distribution is unlimited

THIS PAGE INTENTIONALLY LEFT BLANK

REPORT DOCUMENTATION PAGE			<i>Form Approved OMB No. 0704-0188</i>	
Public reporting burden for this collection of information is estimated to average 1 hour per response, including the time for reviewing instruction, searching existing data sources, gathering and maintaining the data needed, and completing and reviewing the collection of information. Send comments regarding this burden estimate or any other aspect of this collection of information, including suggestions for reducing this burden, to Washington headquarters Services, Directorate for Information Operations and Reports, 1215 Jefferson Davis Highway, Suite 1204, Arlington, VA 22202-4302, and to the Office of Management and Budget, Paperwork Reduction Project (0704-0188) Washington DC 20503.				
1. AGENCY USE ONLY (Leave blank)		2. REPORT DATE June 2013	3. REPORT TYPE AND DATES COVERED Master's Thesis	
4. TITLE AND SUBTITLE THE EFFECTS OF SHOALING INTERNAL TIDES ON BENTHIC EXCHANGE EVENTS AND NEAR-BOUNDARY MIXING ALONG THE CONTINENTAL SHELF			5. FUNDING NUMBERS	
6. AUTHOR(S) Darren L. Pastrana				
7. PERFORMING ORGANIZATION NAME(S) AND ADDRESS(ES) Naval Postgraduate School Monterey, CA 93943-5000			8. PERFORMING ORGANIZATION REPORT NUMBER	
9. SPONSORING /MONITORING AGENCY NAME(S) AND ADDRESS(ES) N/A			10. SPONSORING/MONITORING AGENCY REPORT NUMBER	
11. SUPPLEMENTARY NOTES The views expressed in this thesis are those of the author and do not reflect the official policy or position of the Department of Defense or the U.S. Government. IRB Protocol number ____N/A ____.				
12a. DISTRIBUTION / AVAILABILITY STATEMENT Approved for public release; distribution is unlimited			12b. DISTRIBUTION CODE A	
13. ABSTRACT (maximum 200 words) The effects of shoaling inner shelf internal tidal bores and solitons on the bottom boundary layer have been observed and analyzed during October 2012 at Monterey Bay in Monterey, CA. This research utilized measurements from two different observing systems: the long range propeller-driven AUV called Daphne, and a bottom boundary layer frame measuring changes in temperature, conductivity, pressure, optics, and turbulence during a four week time period. The data collected from these platforms were used to capture the strength of the internal tides and their influence on the bottom boundary layer as they propagate and entrain sediment up into the water column. The focus of this field study, sponsored by the National Science Foundation, was to quantify turbulent intensity levels for active events near the bed and determine correlations with turbulence higher in the water column and the generation of internal nepheloid layers. Typical ϵ dissipation rate values for high turbulent events were $1e-7 \text{ m}^2/\text{s}^3$, and as a result, turbidity levels near the bed increased on average by a third. Observations show how strong changes in the water column currents, turbidity, and turbulence potentially have a large effect on divers and subsurface operating vehicles. Further research is required to provide a predictive capability of this variability.				
14. SUBJECT TERMS Nepheloid Layers, Internal Tidal Bores, Turbulence			15. NUMBER OF PAGES 79	
			16. PRICE CODE	
17. SECURITY CLASSIFICATION OF REPORT Unclassified	18. SECURITY CLASSIFICATION OF THIS PAGE Unclassified	19. SECURITY CLASSIFICATION OF ABSTRACT Unclassified	20. LIMITATION OF ABSTRACT UU	

THIS PAGE INTENTIONALLY LEFT BLANK

Approved for public release; distribution is unlimited

**THE EFFECTS OF SHOALING INTERNAL TIDES ON BENTHIC EXCHANGE
EVENTS AND NEAR-BOUNDARY MIXING ALONG THE CONTINENTAL
SHELF**

Darren L. Pastrana
Ensign, United States Navy
B.S., United States Naval Academy, 2012

Submitted in partial fulfillment of the
requirements for the degree of

MASTER OF SCIENCE IN PHYSICAL OCEANOGRAPHY

from the

**NAVAL POSTGRADUATE SCHOOL
June 2013**

Author: Darren L. Pastrana

Approved by: Prof. Timothy Stanton
Thesis Advisor

Assoc. Prof. William Shaw
Thesis Co-Advisor

Prof. Peter Chu
Chair, Department of Oceanography

THIS PAGE INTENTIONALLY LEFT BLANK

ABSTRACT

The effects of shoaling inner shelf internal tidal bores and solitons on the bottom boundary layer have been observed and analyzed during October 2012 at Monterey Bay in Monterey, CA. This research utilized measurements from two different observing systems: the long range propeller-driven AUV called Daphne, and a bottom boundary layer frame measuring changes in temperature, conductivity, pressure, optics, and turbulence during a four week time period. The data collected from these platforms were used to capture the strength of the internal tides and their influence on the bottom boundary layer as they propagate and entrain sediment up into the water column. The focus of this field study, sponsored by the National Science Foundation, was to quantify turbulent intensity levels for active events near the bed and determine correlations with turbulence higher in the water column and the generation of internal nepheloid layers. Typical ϵ dissipation rate values for high turbulent events were $1\text{e-}7 \text{ m}^2/\text{s}^3$, and as a result, turbidity levels near the bed increased on average by a third. Observations show how strong changes in the water column currents, turbidity, and turbulence potentially have a large effect on divers and subsurface operating vehicles. Further research is required to provide a predictive capability of this variability.

THIS PAGE INTENTIONALLY LEFT BLANK

TABLE OF CONTENTS

I. INTRODUCTION.....	1
A. COASTAL OCEANS	1
1. Monterey Bay	1
<i>a. Tides</i>	<i>3</i>
<i>b. Winds.....</i>	<i>3</i>
<i>c. Stratification</i>	<i>4</i>
B. INTERNAL TIDAL WAVES	5
1. Generation and Nonlinear Propagation	5
2. Internal Nepheloid Layers	7
3. Environmental Impact	8
4. Naval Relevance	8
II. FIELD EXPERIMENT.....	11
A. EXPERIMENT SITE	11
B. INSTRUMENTS	12
1. LRAUV Daphne.....	12
2. Bottom Boundary Layer (BBL) Station	16
<i>a. Acoustic Doppler Current Profiler (ADCP)</i>	<i>17</i>
III. DATA PROCESSING	19
A. LRAUV DAPHNE PROCESSING	19
1. Turbulence Calculations	23
<i>a. Epsilon</i>	<i>24</i>
<i>b. Chi.....</i>	<i>24</i>
<i>c. Turbulent Thermal Diffusivity.....</i>	<i>25</i>
B. BBL FRAME PROCESSING.....	28
1. ADCP	28
IV. RESULTS	31
A. SEDIMENT SUSPENSION.....	31
1. YD 293.04 – 293.12 of Sediment Suspension Event.....	31
2. YD 293.44 – 293.53 of Sediment Suspension Event.....	32
3. YD 293.89 – 293.98 of Sediment Suspension Event.....	33
4. Velocity and Shear during Sediment Suspension Event.....	33
B. NEAR BED TURBULENCE	39
1. Internal Tidal Bore Event.....	39
2. Soliton Events.....	40
V. DISCUSSION.....	51
A. SUSPENDED SEDIMENT EVENTS	51
B. TURBULENCE EFFECTS.....	51
VI. CONCLUSION AND RECOMMENDATION	53
A. SUMMARY.....	53
B. NAVAL IMPACT	54

C. RECOMMENDATIONS FOR FUTURE RESEARCH	54
LIST OF REFERENCES.....	55
INITIAL DISTRIBUTION LIST	59

LIST OF FIGURES

Figure 1.	Bathymetric map of Monterey Bay. The black line represents the shoreline. Elevation scale is shown with blue representing the lowest depths displayed and dark red representing sea level.	2
Figure 2.	Continental shelf sediment composition in percentage of sand off Western California Coast. Monterey Bay is located in the bottom right of the figure (From Edwards 2002).	3
Figure 3.	Illustration of strong northwest winds as they blow over the Monterey Bay coastal waters. As the surface waters move offshore cold, nutrient-rich water moves toward surface (From www.mbari.org).	4
Figure 4.	Internal tidal bore and soliton generation by the lee wave mechanism. (a) An ebb flow across a shelf break causes a depression in the pycnocline. (b) A steep-edged shoreward-propagating bore forms during a slack tide. (c) Leading edge will continue to steepen due to dispersive effects and the internal bore is assisted by the flood tide. (d) The steep leading edge of the bore degenerates into a soliton by the process of the dispersive properties of internal waves. (From Holloway 1987).	7
Figure 5.	Map of the world showing sites where internal solitons have been reported (From Apel 2007).	9
Figure 6.	Map of the Southern Monterey Bay field site, including the deployment locations of the two instruments used in the experiment. The red circle represents the frame's location and the red line shows Daphne's course.	12
Figure 7.	The Daphne AUV that provides new capabilities ranging between propeller driven vehicles, which only have the endurance of about a day, and buoyancy-driven vehicles (gliders), which can operate for months (MBARI photograph).	14
Figure 8.	Turbulence package with covers on all the extremely sensitive microtemperature, microconductivity, and ACM transducers	15
Figure 9.	Fully assembled turbulence package on Daphne with covers removed from the sensors.	16
Figure 10.	Instrumentation on the BBL Frame contains the following: (A) 1.2MHz (left) and 300KHz (right) fast sampling broadband ADCP (B) Hybrid turbulence probes located 0.5 and 1.5 meters above bed (C) BCDVSP that reports at 40Hz, 3-component velocity at 1-cm intervals over 1m range (D) 25cm-path transmissometer	18
Figure 11.	Variations in sea water pressure recognized by Daphne's location relative to the surface of the water. (Top panel) A low-pass filter pressure used to smooth out raw data in order to properly categorize LRAUV movement. (Bottom panel) Illustrates the resultant LRAUV's motion in the water column. During state +1 Daphne is diving, at -1 Daphne is ascending, and at 0 Daphne is changing directions or stationary.	21

Figure 12.	Deployment transit of the LRAUV from 21 OCT to 30 OCT 2013. The two large gaps in the data are due to maintenance being done on the LRAUV out in the bay.	23
Figure 13.	Amplification of the inertial sub range transfer scales. The line from the top left to the bottom right represents a $-5/3$ slope. Large-scale values are represented by epsilon 1 and small-scale values are represented by epsilon 2.	26
Figure 14.	Thermal microstructure gradient spectrum calculated by the microconductivity instruments on board Daphne. The variance of this curve resolves beyond the dissipation rate for chi calculations.....	27
Figure 15.	The local vertical temperature gradients of the four segments surround the bottom-tracking segment. Segment 112 is the bottom-tacking segment and is given a value of the mean to the four gradients averaged together.....	28
Figure 16.	(Top panel) The cross-shelf or U component of velocity of the BBL frame. East is represented by the positive values in red and West is negative and in blue. (Middle panel) The along-shore (N or S) or V component of velocity. North is positive and red and south is negative and blue. (Bottom panel) Calculated backscatter using the sonar equation.....	29
Figure 17.	(Top panel) Current speeds in meters per second with red representing max speed and blue represents still water. (Middle panel) Vector differential of current represented by shear. (Bottom panel) Time series of shear at 6m HAB.....	30
Figure 18.	Suspended sediment event: YD 293.04 -293.12. Solid black vertical line represents the positioning of the frame as Daphne transits the shelf. The curved black line is the bathymetry of Monterey Bay. (Panel 1) Temperature of the water column as Daphne transits onshore. (Panel 2) Turbidity seen by Daphne as it propagates through the water column. (Panel 3) turbidity seen near the seafloor by the 1200KHz ADCP of the frame.....	35
Figure 19.	Suspended sediment event: YD 293.44-293.53. Solid black vertical line represents the positioning of the frame as Daphne transits the shelf. The curved black line is the bathymetry of Monterey Bay. (Panel 1) Temperature of the water column as Daphne transits onshore. (Panel 2) Turbidity seen by Daphne as it propagates through the water column. (Panel 3) turbidity seen near the seafloor by the 1200KHz ADCP of the frame.....	36
Figure 20.	Suspended sediment event: YD 293.89-293.98. Solid black vertical line represents the positioning of the frame as Daphne transits the shelf. The curved black line is the bathymetry of Monterey Bay. (Panel 1) Temperature of the water column as Daphne transits onshore. (Panel 2) Turbidity seen by Daphne as it propagates through the water column. (Panel 3) turbidity seen near the seafloor by the 1200KHz ADCP of the frame.....	37
Figure 21.	BBL Frame instruments covering sediment suspension event YD 293.04-293.98. (Panel 1 and 2) Velocity (u and v) magnitudes propagating over	

	300KHz ADCP. (Panel 3) Time series of backscatter from 1200KHz ADCP. (Panel 4) Shear values calculated from u and v velocity component of 300KHz ADCP. (Panel 5) Time series of calculated shear values at 5m HAB.....	38
Figure 22.	Offshore transit of Daphne section number 76. (Panel 1) Lateral view of the LRAUVs movements throughout the water column with segment numbers over the bottom tracking segments. (Panel 2) Temperature observed. (Panel 3) OBS from Daphne. (Panel 4-6) Turbulence calculations for epsilon, chi, and K_T	42
Figure 23.	Thermal microstructure gradient spectrum calculated by the microconductivity instruments on board Daphne of each bottom-tracking segment over section number 76. Colors correlate with previous figure of the same offshore transit section.	43
Figure 24.	Offshore transit of Daphne section number 64. (Panel 1) Lateral view of the LRAUVs movements throughout the water column with segment numbers over the bottom tracking segments. (Panel 2) Temperature observed. (Panel 3) OBS from Daphne. (Panel 4-6) Turbulence calculations for epsilon, chi, and K_T	44
Figure 25.	Thermal microstructure gradient spectrum calculated by the microconductivity instruments on board Daphne of each bottom-tracking segment over section number 64. Colors correlate with previous figure of the same offshore transit section.	45
Figure 26.	Offshore transit of Daphne section number 74. (Panel 1) Lateral view of the LRAUVs movements throughout the water column with segment numbers over the bottom tracking segments. (Panel 2) Temperature observed. (Panel 3) OBS from Daphne. (Panel 4-6) Turbulence calculations for epsilon, chi, and K_T	46
Figure 27.	Thermal microstructure gradient spectrum calculated by the microconductivity instruments on board Daphne of each bottom-tracking segment over section number 76. Colors correlate with previous figure of the same offshore transit.....	47
Figure 28.	Offshore transit of Daphne section number 80. (Panel 1) Lateral view of the LRAUVs movements throughout the water column with segment numbers over the bottom tracking segments. (Panel 2) Temperature observed. (Panel 3) OBS from Daphne. (Panel 4-6) Turbulence calculations for epsilon, chi, and K_T	48
Figure 29.	Thermal microstructure gradient spectrum calculated by the microconductivity instruments on board Daphne of each bottom-tracking segment over section number 80. Colors correlate with previous figure of the same offshore transit.....	49

THIS PAGE INTENTIONALLY LEFT BLANK

LIST OF TABLES

Table 1.	Segment definition for the LRAUV's transit through the water column. The left most column is the different 'state' numbers for the LRAUV. The center column is a description of each state and the far right column is the direction of Daphne transiting through the water column.....	22
----------	---	----

THIS PAGE INTENTIONALLY LEFT BLANK

LIST OF ACRONYMS AND ABBREVIATIONS

PISCO	Partnership for Interdisciplinary Studies of Coastal Oceans
ISW	Internal Solitary Waves
ITB	Internal Tidal Bores
CODE	Coastal Ocean Dynamics Experiment
N^2	Brunt-Visailla Frequency
INL	Intermediate Nepheloid Layers
SOF	Special Operation Forces
NPS	Naval Postgraduate School
LRAUV	Long Range Autonomous Underwater Vehicle
MBARI	Monterey Bay Aquarium Research Institute
NSF	National Science Foundation
CTD	Conductivity Temperature Depth
ACM	Acoustic Current Meter
BBL	Bottom Boundary Layer
ADCP	Acoustic Doppler Current Profiler
BCDVSP	Biostatic Coherent Doppler Velocity and Sediment Profiler
HAB	Height Above Bed
OBS	Optical Backscatter Sensor

THIS PAGE INTENTIONALLY LEFT BLANK

ACKNOWLEDGMENTS

I would first like to thank my advisor, Professor Tim Stanton, for his motivation, support, and above all, believing in my abilities to work through an incredible data collection. Professor Stanton provided me with the hands-on opportunity for deployment and recovery of the bottom boundary layer frame to the experimental site. I am grateful for his inspiration in becoming passionate about research and the value in data processing.

I would also like to give a special thanks to my co advisor, Bill Shaw, and the rest of the NPS Turbulence Group. Without their support and patience helping me understand and debugging my MATLAB code, I would not have been successful in completing my research. In addition, I would like to thank the Undersea Warfare department, especially Rear Admiral (RET) Richard Williams and Rea Admiral (RET) Jerry Ellis, for allowing me the opportunity to join their diverse program while studying at NPS.

I will remain forever grateful for the love and care shown to me by my family: Ron, Anita, Kimberly Pastrana, as well as my girlfriend ENS Kierstin King. They were always there helping me keep things in perspective and they had a special way of putting a smile on my face. In addition, I would like to thank MAJ Brandon Gebhardt and ENS Mike Martin for sharing and providing the necessary down time on the weekends after long weeks.

Above all, I could not have completed this thesis without God's agape love for me. He continues to provide blessings of patience, willpower, and strength to push through life's challenging moments.

THIS PAGE INTENTIONALLY LEFT BLANK

I. INTRODUCTION

A. COASTAL OCEANS

Vigorous productivity in the coastal oceans can be linked to areas of strong coastal upwelling. Rich nutrient coastal waters provide habitats for more than 90% of all marine organisms (PISCO 2009). Regions of upwelling along the coast are essential to maintaining ocean productivity due to the injection of nutrients into the upper water column (Cazenave et al. 2011). In addition to strong upwelling, coastal oceans are constantly affected by tides, winds, and stratification. Combinations of these forcing mechanisms acting on the water column play a significant role in the generation of internal solitary waves (ISWs) within coastal oceans. McPhee-Shaw (2007) study shows how shoaling internal waves are also a vital instrument for transporting nutrients to inner shelf kelp ecosystems. As Internal Tidal Bores (ITBs) propagate on shore across a continental shelf into shallower waters it interacts with the sloping topography. Steep changes in topography increase near bed shear and slow down the shoaling wave causing the wave itself to steepen resulting in nonlinear effects including the production of leading solitons ahead of the internal tidal bore. Nonlinear internal solitary waves influence numerous scientific areas containing cross-shore transport along the shelf, ocean acoustic propagation, coastal engineering, and biological oceanography (Farmer and Armi 1999).

1. Monterey Bay

Monterey Bay is positioned along the Central California Coast between 35° - 37° N Latitude and 121° - 123° W Longitude (Figure 1). The Bay is a major location for examining and studying internal tide activity due to the underwater topography and coastal ocean processes. Typical continental shelves are defined as the area of the ocean floor between 30 and 200 meters deep. The continental shelf of Monterey Bay is relatively broad for the US West Coast, about 20km wide. A significant portion of the shelf's sediment type is composed of mud, fine silt, and clay and their percentages

increase toward the shelf break (Figure 2). The shelf break is typically found to be about one hundred meters off shore.

A deep submarine canyon bisects Monterey Bay's continental shelf. As the Monterey Bay Canyon splits through the middle of the continental shelf, it generates steep ridges and areas of sloping, irregular bathymetry. The largest slopes within the canyon are located at the southern edge where depths change on the order of one thousand meters over a distance of five thousand meters. Monterey Bay Canyon terminates within one hundred meters of the shore at the eastern end of the bay. Several studies have been conducted to determine the effects on internal tides within the canyon (Petruncio et al. 1998). The shelf is frequented by energetic non-linear internal waves and is typically a coastal upwelling environment from spring until summer (Cazenave et al. 2011).

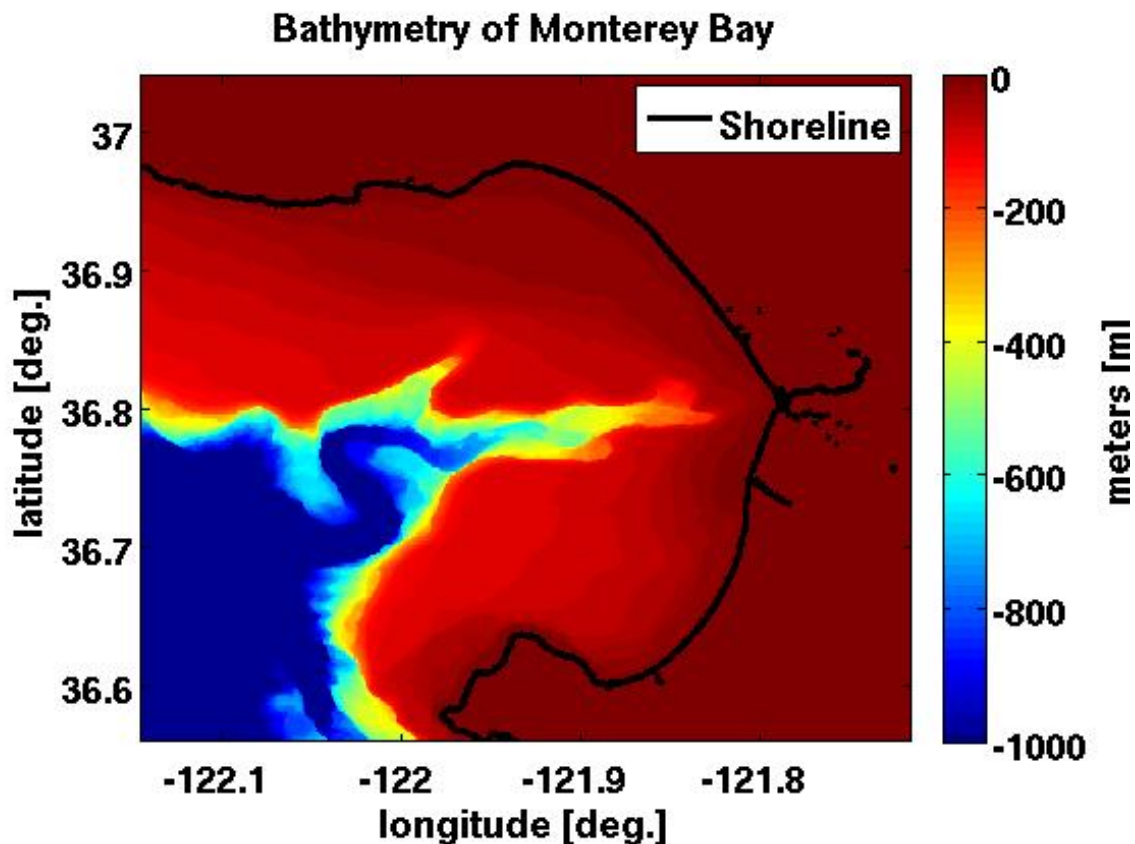


Figure 1. Bathymetric map of Monterey Bay. The black line represents the shoreline. Elevation scale is shown with blue representing the lowest depths displayed and dark red representing sea level.

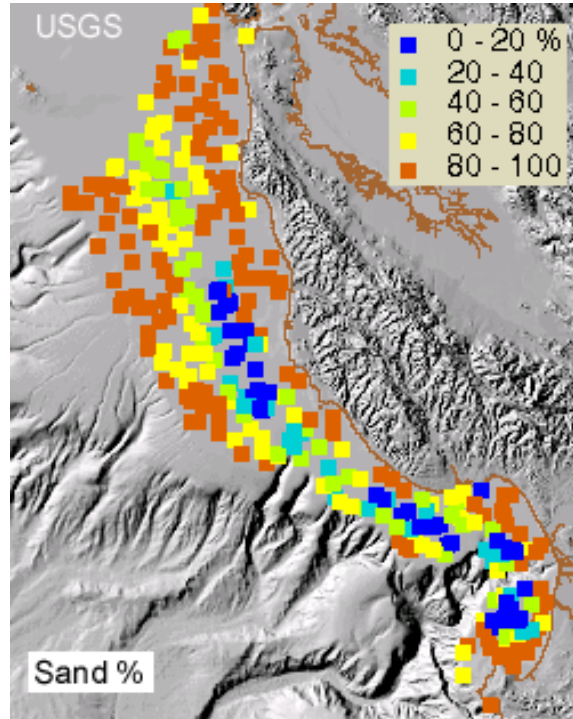


Figure 2. Continental shelf sediment composition in percentage of sand off Western California Coast. Monterey Bay is located in the bottom right of the figure (From Edwards 2002).

a. Tides

The tides in Monterey Bay are mixed, with lunar, M_2 , semi-diurnal being the dominant tide. Therefore, the lunar tide is the likely source for tidally driven nonlinear internal wave generation. Over the Northern California continental shelf, during the 1982 upwelling season as part of the Coastal Ocean Dynamics Experiment (CODE), comparisons with the internal wave theory showed the observed vertical and horizontal structure of the semidiurnal band horizontal current and temperature fluctuations to be consistent with a first baroclinic mode internal wave with a horizontal wavelength of 20-30km (Rosenfeld 1990).

b. Winds

During the spring and summer months in Monterey Bay, strong north-westerly winds affect coastal upwelling and advection of the water in the bay (Figure 3). Over this time period, maximum wind stress is toward the equator off the coast of

California leading to strong seasonal upwelling in Monterey Bay (Hickey 1998). However, winter storms disrupt normal wind patterns and lower the mixed layer in the water column resulting in less upwelling. Opposing southwesterly winds along the coast cause a northward surface current shoreward of the California Current called the Davidson Current. The opposing Davidson Current impedes the transport of cold fresh water from the north. Consequently, local wind patterns and the direction of the surface currents have a significant impact on the stratification in shallow water columns.

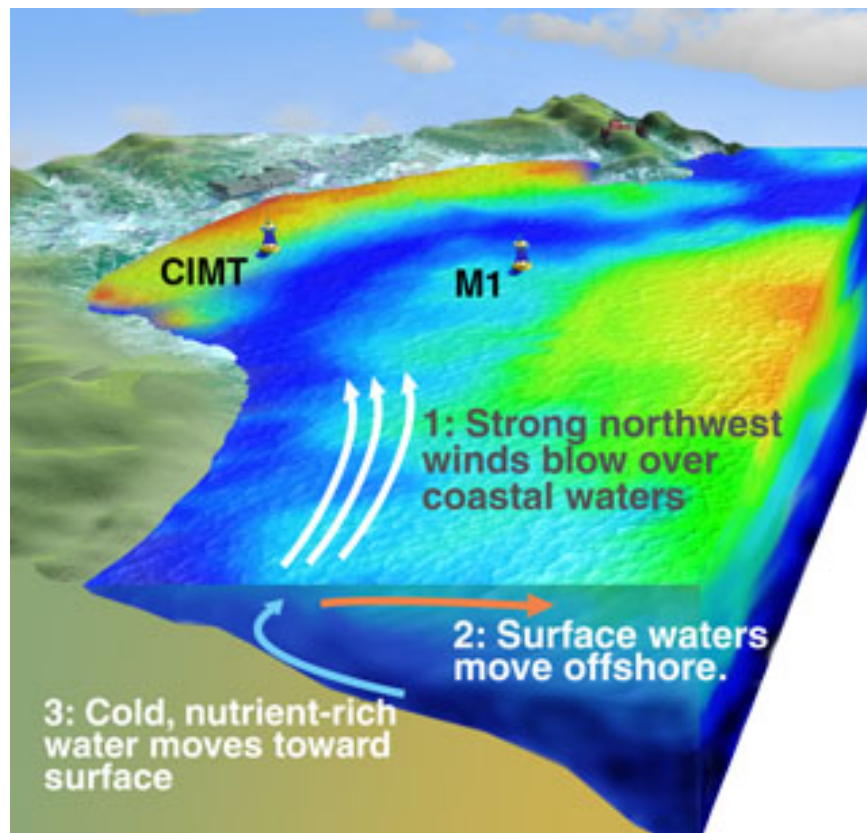


Figure 3. Illustration of strong northwest winds as they blow over the Monterey Bay coastal waters. As the surface waters move offshore cold, nutrient-rich water moves toward surface (From www.mbari.org).

c. Stratification

Stratification varies seasonally within the Monterey Bay. Hickey (1998) observed that stratification in California coastal areas are controlled by large-scale advection and upwelling of water masses. During periods of upwelling, cool water is

pumped onto the continental shelf along the ocean floor resulting in near surface stratification. In the spring and summer months, when upwelling is the strongest, a predominate two layer system is created in the water column. Strong stratification, expressed as large buoyancy frequencies, in Monterey Bay results in an increase of internal tide activity and, more specifically, internal bore activity. The buoyancy or Brunt-Visailla frequency (N^2),

$$N^2 = -\frac{g}{\rho} \frac{\partial \rho}{\partial z} \quad (1)$$

is the measure of static stability in the ocean, where g is gravity, ρ the local density. Small N^2 values indicate weak stratification while large N^2 values indicate strong stratification. Past studies have shown that near-surface shelf stratification and increased maximum buoyancy frequencies exist during late summer months in Monterey Bay (Crabbe 2007). These conditions arise because of low to moderate amplitude winds, diurnal afternoon sea breeze, few storms, and strong solar heating of the surface layer during late summer. Spatially continuous strong stratification across the shelf is and high necessary for the shoreward propagation of the internal tide into the coast.

B. INTERNAL TIDAL WAVES

1. Generation and Nonlinear Propagation

Internal tides are tidally generated internal waves generated as barotropic tidal currents flow over sloping topography. Internal tides are commonly observed at continental slopes or breaks, straits, and sills within the ocean. Typical internal tides that propagate over the continental shelf have current speeds between 5-20 cm s^{-1} and isopycnal displacement amplitudes between 20-50 m (Huthnance 1989; Foreman 1995).

One of the common observed generation mechanisms for internal tides at the continental shelf break is called the lee-wave mechanism (Holloway 1987). During lee-wave formation, a depression in the pycnocline is formed when ebbing tidal waters cross over a bottom feature or shelf break (Figure 4). As a result, the depressed isopycnals generates a standing lee wave of depression. When the flow ceases during the slack tide, the wave of depression begins to propagate both onshore and offshore. The offshore

propagation of the wave travels into deep waters where it dissipates with little change to the water column. On the other hand, as the onshore wave starts to propagate it shoals, becomes nonlinear, and begins self-advection. Self-advection causes waves with larger amplitudes to move faster. Therefore, the onshore propagating wave gets steeper, often forming a bore-like wave called an internal tidal bore. As the ITB continues to propagate shoreward, the subsequent flood tide will assist in the propagation process. Under strong stratification conditions, the steep leading edge can generate bore-like shockwaves that form a series of depressions in the water column ahead of the ITB. These depressions are commonly referred to as internal tidal solitons (Noble et al. 2009). The formation of solitons depends on the existence of both intrinsic dispersion and nonlinearity in the medium (Apel et al. 2007). The magnitude and energy of the soliton are increased as the internal tidal bore continues to propagate onshore. In summary, as ocean tides ebb and flow over the continental shelf, some of the barotropic tidal kinetic energy is converted to baroclinic kinetic energy through the disturbance of the vertical density structure in the water column, which may cause internal bores of pulse-like density displacements commonly referred to as solitons (Ostrovsky and Stepananyans 1989; Stanton and Ostrovsky 1998).

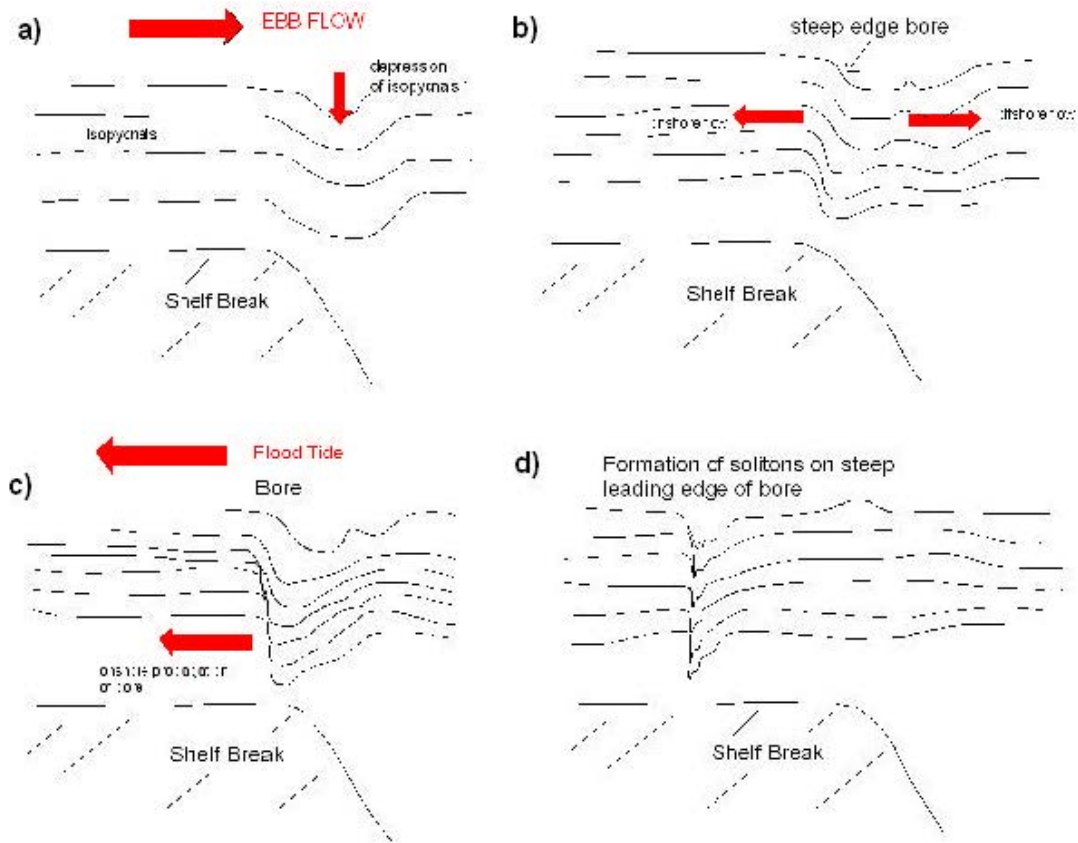


Figure 4. Internal tidal bore and soliton generation by the lee wave mechanism. (a) An ebb flow across a shelf break causes a depression in the pycnocline. (b) A steep-edged shoreward-propagating bore forms during a slack tide. (c) Leading edge will continue to steepen due to dispersive effects and the internal bore is assisted by the flood tide. (d) The steep leading edge of the bore degenerates into a soliton by the process of the dispersive properties of internal waves. (From Holloway 1987).

2. Internal Nepheloid Layers

Internal nepheloid layers (INLs) are layers of elevated suspended particulate material within the water column. INLs are observed commonly near continental slopes and shelves, although little is known about their formation mechanism and dispersion rates. One hypothesis is that the creation of such layers may form by strong baroclinic tidal currents that create elevated turbulence along a critical slope and can suspend sediments into the water column (McPhee-Shaw et al. 2004). Previous to MCPhee-Shaw's laboratory experiment that found intrusions most intense at supercritical sloping

conditions, INLs were thought to occur with the critical reflection of semidiurnal internal tides. Puig's (2004) observations further supports McPhee-Shaw's discovery by finding nepheloid layers near critical angles on the northwestern Alboran slope, southwest Mediterranean Sea, mainly around depths of 200m to 500m.

In Monterey Bay, nonlinear internal waves transport sediment offshore (Carter et al. 2005). Johnston et al. (2011) observed, through their phase-averaged measurements of INLs and currents in Monterey Bay, internal wave-driven westward transport of sediment. The study concluded the variable INL locations in depth and latitude suggest mesoscale variability alters the conditions at the shallower shelf generation site or along the propagation path of the internal tide. Along the Monterey Bay Shelf, intrusions can extend 10-20km offshore propagating at a maximum rate of one km per 3.5 hours (McPhee-Shaw 2002; Cazenave et al. 2011).

3. Environmental Impact

Internal tidal waves and solitons could have a major effect on biogeochemical cycles and global climate in coastal oceans. Harmful algal bloom species have a benthic resting state and may be the cause of toxic blooms when the dormant cells are carried up into the water column through a process called benthic-interior exchange (Rines et al. 2002; McManus et al. 2007). Benthic exchange could explain a general correspondence between increased levels of Chlorophyll-a and shelf width in major upwelling areas (Patti et. al. 2008). In addition to harmful algal bloom, internal tidal waves may significantly contribute to energy dissipation, and, therefore, ocean mixing and global climate (Baines 1982).

4. Naval Relevance

The United States Navy, particularly the submarine and Special Operation Forces (SOF) communities, has taken special interest in any field of research that has a direct effect on mission success in order to maintain theatre dominance. A majority of submarine and SOF operations are executed in the Coastal Ocean environment where ISWs are ubiquitous (Figure 5). Critical to the operation of submarines and other underwater vehicles is the crew's ability to utilize acoustic propagation. Consequently, internal waves and solitons produce strong "scintillation" in acoustic wave propagation

and therefore can hamper the operator's ability to use underwater acoustics (Kantha et al. 2000). Apel et al. (2007) also discusses the effect of internal waves and solitons on sound wave propagation. Results from their research show ISWs influence propagation of acoustic signals in water and may form specific conditions for ducting sound waves.

In addition to underwater vehicle operations, countermining operations are also effected by ISWs. Mines can physically be moved or altered during ISW events. Navy Divers and Explosive Ordinates Disposal team members diving on a coastal mission can have their visibility altered by the presence of INLs. Thus, the United States Navy has a high interest in understanding and predicting coastal tide-forced internal wave activity that could affect the outcome of their mission.

The intelligence preparation of the environment is critical for operational success, whether the need is halfway around the world or in U.S. coastal waterways, ports, and rivers (Sandel 2009). It is essential to gather oceanographic data before conducting naval operations in order to provide information on currents, internal waves, and bottom geophysical parameters, to deem an area safe to carry out a mission (Dept. of Navy 2004). A strong understanding of coastal oceanographic processes can better equip naval officers in the implementation of naval objectives, and therefore can significantly alter the outcome of a mission.

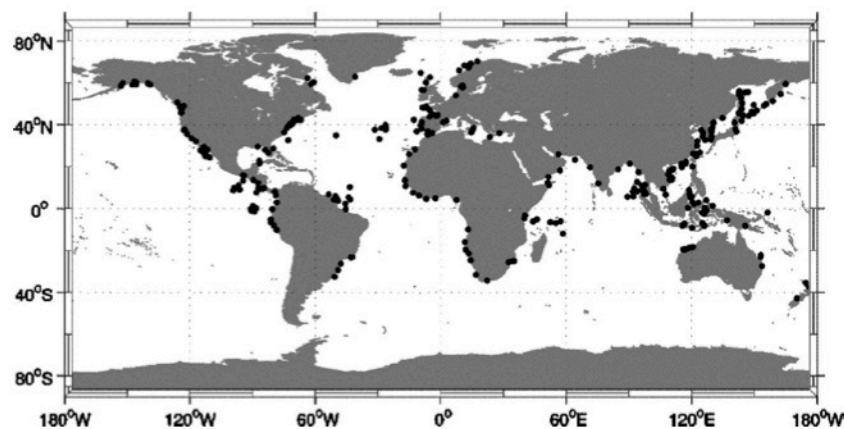


Figure 5. Map of the world showing sites where internal solitons have been reported (From Apel 2007).

THIS PAGE INTENTIONALLY LEFT BLANK

II. FIELD EXPERIMENT

The Naval Postgraduate (NPS) Ocean Turbulence Group, Moss Landing Marine Lab and Monterey Bay Aquarium Research Institute (MBARI) combined their efforts and technology in order to collect data over the continental shelf in Monterey Bay in a series of three experiments. The observations were collected as part of the National Science Foundation (NSF) study on benthic exchange events and near boundary mixing along the continental shelf.

A. EXPERIMENT SITE

The Monterey Bay shelf is an ideal site for the experimental study of temporal and spatial development of internal tidal bores and nepheloid layers. Steep continental shelf breaks are one of the main features in the bay that provide a suitable location for internal tide generation. Mud and fine sediments make up the bottom type of the bay dominantly, which aids in the generation of nepheloid layers. Monterey Bay's wide shelf supports "mud belt" deposits from winter storm runoffs from local rivers and streams. These characteristics of the Monterey Bay shelf are similar to those found on shelves throughout the world ocean, indicating that knowledge gained from process studies in Monterey Bay can be applied widely.

Observations in this thesis were gathered from two main instrument systems, a bottom boundary layer (BBL) frame and a long-range autonomous underwater vehicle (LRAUV), Daphne, from a process study on the southern Monterey Bay Shelf during the month of October 2012. The two systems are described in further detail in the following section. The frame was deployed on 1 OCT 2012 at $36^{\circ} 42' 51''$ N and $121^{\circ} 51' 69''$ W in a water depth of 63 meters (Figure 6). On 11 OCT 2012, Daphne was deployed and operated along a line between $121^{\circ} 49' 47''$ - $121^{\circ} 51' 69''$ W longitude along the $36^{\circ} 42' 57''$ N latitudinal line. The frame was recovered after twenty days of data collection on 21 OCT 2012 while the Daphne remained in the water until 30 OCT 2012. During the month long data collection, Daphne and the frame were both operational for a ten-day period from 11 OCT–21 OCT 2012.

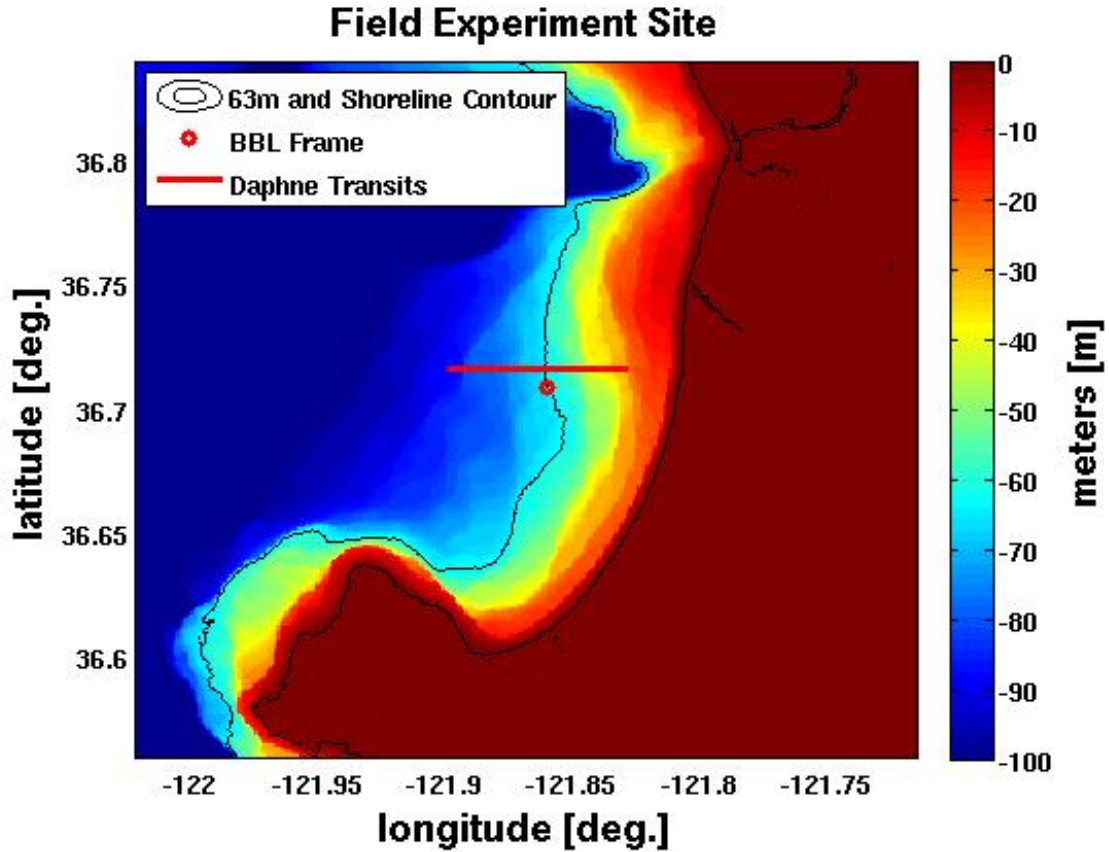


Figure 6. Map of the Southern Monterey Bay field site, including the deployment locations of the two instruments used in the experiment. The red circle represents the frame's location and the red line shows Daphne's course.

B. INSTRUMENTS

1. LRAUV Daphne

Over the past several years, engineers in J. Bellingham's group at MBARI have developed and advanced a new class of long range AUVs to support physical, chemical, and biological sensing missions. Such missions have the endurance capability of spanning over 1,000 kilometers or more (MBARI 2013). The LRAUV operate at speeds around one meter per second and with minimal sensors allowing the vehicle to range over several thousand kilometers. The long endurance capabilities of MBARI's new vehicle, Daphne (Figure 7), allows observations over the entire continental shelf for a period of ten to twenty days, which covers over half of the fortnightly tidal cycle. Daphne's dead reckoning navigation is effective at maintaining a set transect in combination with

transect end-point surface GPS fixes. Daphne corrects any deviations to the intended course when the LRAUV surfaces and receives its current GPS fix.

Daphne is relatively easy to handle, about 120 kilograms dry weight, and designed to be simple enough for operations by individual laboratories. The forward bow section of Daphne is free-flooded and houses the scientific payload including the Conductivity Temperature Depth (CTD) and three optical sensors. The CTD provides regional descriptions of the oceanographic area's temperature, and salinity, while the LRAUV transits through the water column. Fluorometers, one of the three optical sensors, are sensitive to biological backscatter and therefore detect the presence of chlorophyll in the water column. In addition to the fluorometer, there are 470 nm and 650 nm optical backscatter sensors that measure particle suspension of benthic material near the seabed. The data analyzed from the three optic sensors are used to generate high-resolution time series of the water column optical properties. Furthermore, the sensors are used to classify when and where on the continental shelf a nepheloid layer formation was present. Daphne provides the ability to map boundary layer detachment in cross-shelf sections, resolving scales from bottom boundary layer turbulent eddies to full-water column depth, and width of the shelf (McPhee-Shaw 2002).

For the benthic exchange NSF project, the NPS Turbulence Group attached a custom designed and fabricated turbulence package at the front of the LRAUV (Figures 8-9). Included in the turbulence package are microconductivity, microtemperature, and Acoustics Current Meter (ACM) transducers. These fast-response instruments are used to resolve a wide spatial range of turbulent fluctuations present in the water column. Specifically, the microconductivity instrument is constructed of two needles 2mm apart from one another. An AC voltage is sent through the needles to measure the AC current in the water, to measure conductivity in the water. The microtemperature instrument measures the temperature of the water column directly. Time response for the instrument is .007 seconds and has a cutoff frequency of 22.73 Hz. Eight ACM transducers are paired at a distance of 20cm on paired rods. Each pair of transducer measures a different component of velocity, u , v , or w . In this thesis, the turbulence measurements will be used to calculate near-bed dissipation rate of kinetic energy and scalar variance.



Figure 7. The Daphne AUV that provides new capabilities ranging between propeller driven vehicles, which only have the endurance of about a day, and buoyancy-driven vehicles (gliders), which can operate for months (MBARI photograph).

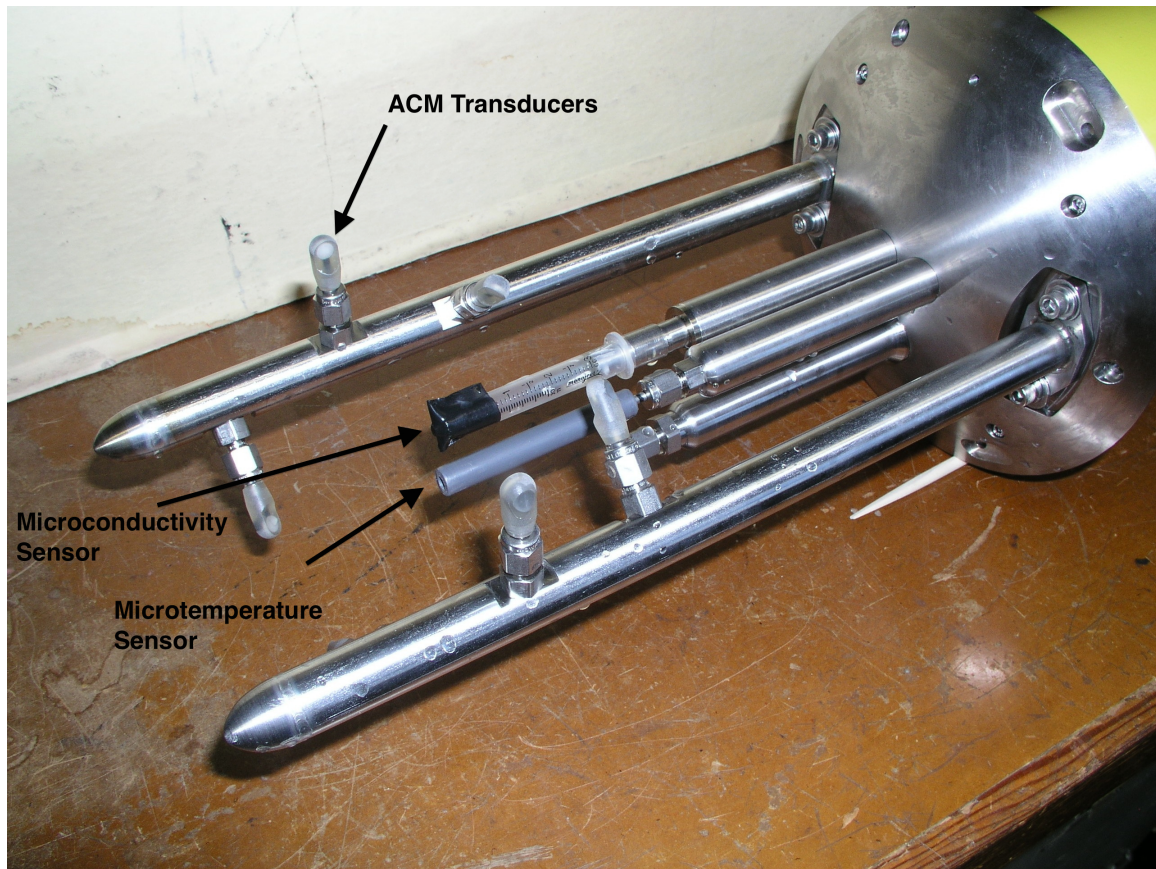


Figure 8. Turbulence package with covers on all the extremely sensitive microtemperature, microconductivity, and ACM transducers



Figure 9. Fully assembled turbulence package on Daphne with covers removed from the sensors.

2. Bottom Boundary Layer (BBL) Station

The NPS Turbulence Group, led by Tim Stanton and William Shaw, have assembled an instrumented frame (Figure 10) designed to measure stresses, bed entrainment processes, and fine sediment fluxes both vertically and laterally at the bottom boundary layer of the seafloor. On deployment, the frame was aligned with its long axis alongshore to lessen the effects of frame-wake disturbances generated by the cross-shore wave motions. Instrumentation on the frame includes 1.2MHz (0.5m vertical resolution) and 300KHz (2m vertical resolution) Acoustic Doppler Current Profilers (ADCP), two hybrid turbulence probes that measure at 0.5m and 1.5m above the bed, a Bistatic Coherent Doppler Velocity and Sediment Profiler (BCDVSP) reporting at 40Hz with 1cm vertical resolution, and a 25cm-path transmissometer. The turbulence instrument packages are designed to directly measure vertical turbulent fluxes and turbulent

diffusivity using both scalar-dissipation and eddy-correlation techniques. It is possible to use the dissipation technique where turbulence is weak, while the eddy-correlation method measure fluxes during strong mixing events near the bed. In this thesis I will focus on the dissipation techniques.

a. Acoustic Doppler Current Profiler (ADCP)

The ADCP measures current velocity profiles by transmitting sound pulses through the water column along four narrow, upward-directed beams. The sound scattered off particles within the water column are received and the beam velocities of the scatters relative to the ADCP result in Doppler shifts of the returning sound energy to each ADCP transducer. Transducer quality is vital for data worth. These transducers must be directional and efficient in order to process receive the very weak backscattered energy. Along-beam current velocities are then calculated using the Doppler shift. In order to obtain the orientation of the transducers, an internal compass and tilt sensors were measured in both ADCPs.

By examining the ADCP's echo intensity, the effective range for the ADCP can be determined. Echo intensity is a measure of the signal strength of the echo returning from the ADCP's transmitted pulse. When a constant low value is found for several bins, the backscatter profile indicates that the ADCP noise floor has been reached. Beyond this range, the ADCP cannot accurately calculate Doppler shifts (RD Instruments 1998). The Echo intensity from the ADCP also provides a measure for the density of water particles suspended in the water column, which is used in this thesis to estimate suspended sediment levels in the interpretation of the LRAUV data.

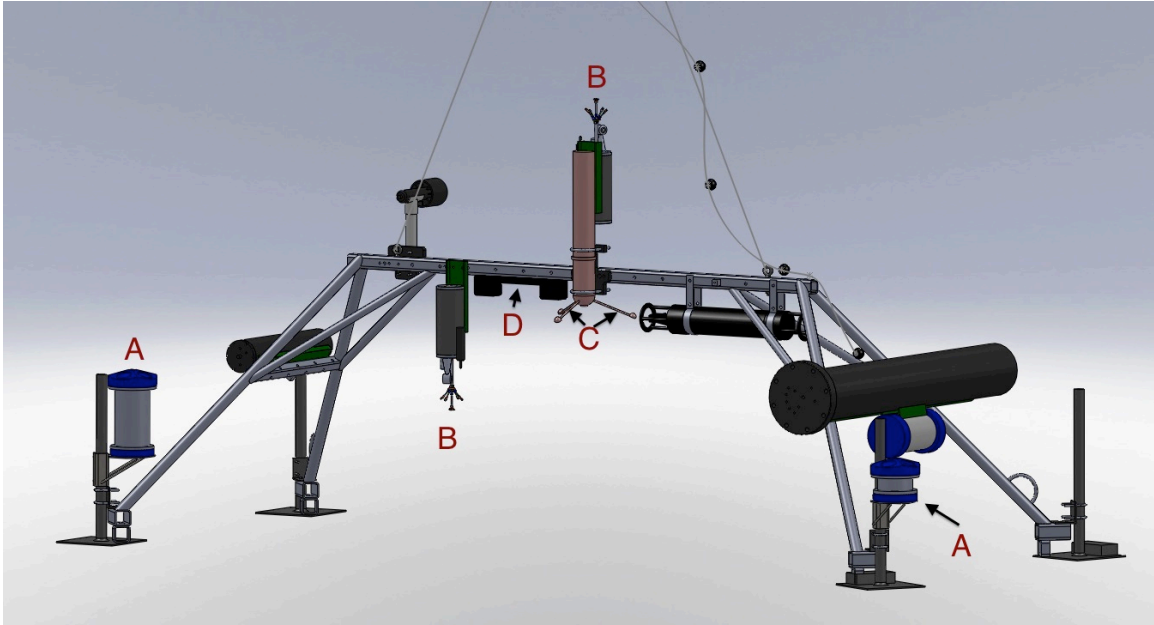


Figure 10. Instrumentation on the BBL Frame contains the following: (A) 1.2MHz (left) and 300KHz (right) fast sampling broadband ADCP (B) Hybrid turbulence probes located 0.5 and 1.5 meters above bed (C) BCDVSP that reports at 40Hz, 3-component velocity at 1-cm intervals over 1m range (D) 25cm-path transmissometer

III. DATA PROCESSING

A. LRAUV DAPHNE PROCESSING

Once Daphne was pulled out of the water following the field experiment, the MBARI team off-loaded the raw data and information stored by Daphne's instruments and converted them into Matlab data files.

The raw data were then extracted and sorted into profiles, bins, sections, and segments in order to generate temporal and spatial views of the water column across the shelf. During the field experiment, Daphne traveled between two prescribed longitudinal coordinates transiting either nominally offshore or onshore. The onshore transit consisted of profiles over the entire water column, as the LRAUV would start at the surface and dive down to the bed before returning back to the surface. On the offshore transit, the LRAUV dove down to a depth of six meters height above bed (HAB) where it remained for 500m offshore distances. At the end of each 500m stretch, Daphne would conduct a mini profile up into the water column of approximately twenty meters HAB, to sample the near-bed gradients of scalar properties.

Over the course of each transit the LRAUV was diving, surfacing, or changing directions. In order to analyze the water column properties and locate internal tide events, it is necessary to break down and classify the LRAUV's movements, called segments, in order to form profiles or timeseries elements for each transect analyze the water column structure and locate internal tide events. Large on-shore profiles, called sections or transects, conducted by Daphne resolve water column structure. After the segmenting process is complete, the data go through a binning program so the depth of the collected data in water column can be distinguished. On the other hand, the bottom tracking movement during the offshore sections are used to calculate the turbulence levels near the bed.

A low-pass-filtered, temporal derivative of pressure, which was gathered throughout the experiment, was used to determine Daphne's mode of travel and break the raw data into segments. The low pass filter was used in order to avoid having small

fluctuations in seawater pressure produces erroneous segment breaks (Figure 11). For each of the data record segments Daphne was assigned an indexing number or state variable to keep track of its movement (Table 1).

As soon as the data segments were assigned state variables, they could be put through the segmenting process. A segment is the portion of data collected while the LRAUV transits during a specific state. For example, the first segment is when Daphne began its initial decent through the water column, state 1 from table, until it changes direction to begin its rise through the water column. For each segment variables such as start and stop times, latitude and longitude, and HAB calculations are stored. After the program is finished running in Matlab, the output is a mat file containing the indexing data for specific segmented states.

Once the segments program was completed, another script was written in order to vertically bin the timeseries data for each segment. Binning the data is done in one-meter increments starting from the deepest depth of the LRAUV's transit to the surface of the water column. Profiles can then be constructed by compiling the vertical bins together in order to cover the entire water column. After individual profiles are created, they are then combined into sections, which represent a complete transect either offshore or onshore of the LRAUV. During the deployment, Daphne was interrupted twice for recharging and sensor refurbishment, which is seen as the gaps to Figure 12. In all, Daphne's data set consists of eighty-eight sections over the twenty-day deployment. These profile transect timeseries define the evolution of the water column and help draw focus to specific days of interest with intensified activity.

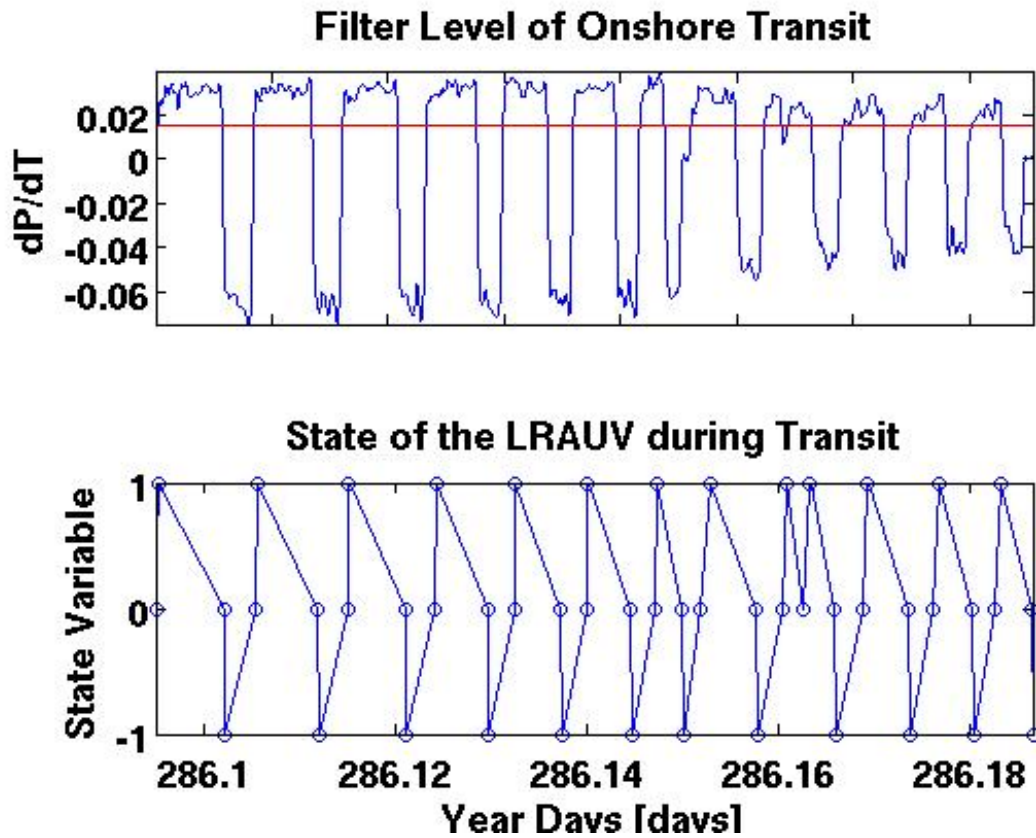


Figure 11. Variations in sea water pressure recognized by Daphnes location relative to the surface of the water. (Top panel) A low-pass filter pressure used to smooth out raw data in order to properly categorize LRAUV movement. (Bottom panel) Illustrates the resultant LRAUV's motion in the water column. During state +1 Daphne is diving, at -1 Daphne is ascending, and at 0 Daphne is changing directions or stationary.

AUV Number Assignment	Description	Primary Direction of Travel
0	Change of direction or unnecessary movement	Either
1	Diving in the water column over 20m	On-Shore
-1	Surfacing in the water column over 20m	On-Shore
2	Near bed transit	Off-Shore
3	Diving in the water column less than 20m	Off-Shore
-3	Surfacing in the water column less than 20m	Off-Shore

Table 1. Segment definition for the LRAUV's transit through the water column. The left most column is the different 'state' numbers for the LRAUV. The center column is a description of each state and the far right column is the direction of Daphne transiting through the water column.

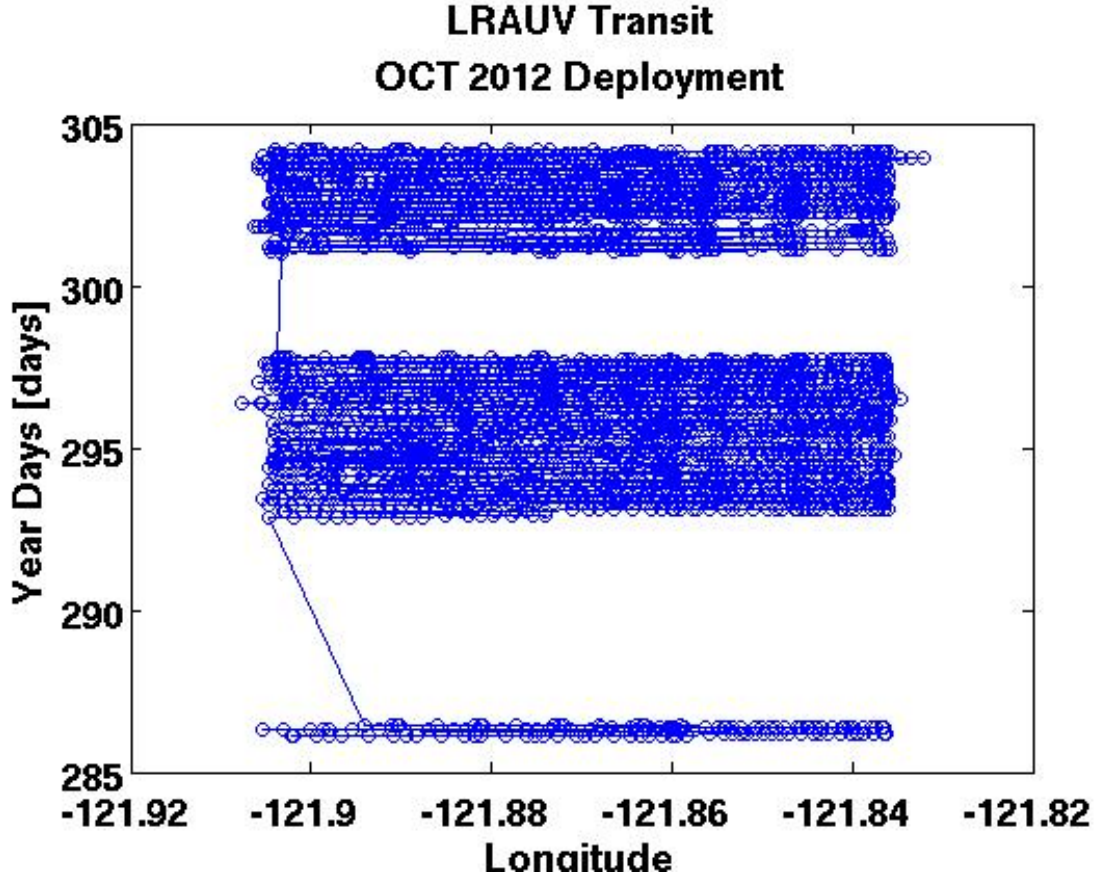


Figure 12. Deployment transit of the LRAUV from 21 OCT to 30 OCT 2013. The two large gaps in the data are due to maintenance being done on the LRAUV out in the bay.

1. Turbulence Calculations

After the segmenting and binning of the raw LRAUV data was completed, turbulence calculations for ϵ (epsilon), χ (chi), and K_T (turbulent thermal diffusivity) were made for all number two segments. These bottom-tracking segments are assumed to provide the best data collection for determining the turbulence near the bed. Ultimately, the calculated turbulent values should reveal bottom mixing associated with features such as passing internal tidal bores and or solitons. Unfortunately, floating matter in the water column such as jellyfish or seaweed can contaminate the high-resolution instruments making the data unusable.

a. Epsilon

Epsilon represents the turbulent kinetic energy dissipation rate, with units of m^2s^{-3} . The definition for ϵ was formulated by interpreting the friction term in the momentum equation after multiplying through by its velocity component resulting in a term equal to:

$$3\nu\left(\frac{\partial u'}{\partial z}\right)^2 \quad (2)$$

where ν is the viscosity and u' is the fluctuation velocity along a single component. Epsilon represents the loss of turbulent kinetic energy due to friction at small scales. Its numerical value is large in the presence of turbulence and can be calculated from the inertial subrange part of the wave number spectrum of the ACM vertical velocity measurement on the LRAUV.

The inertial sub range transfer scale is seen when the wavenumber has a slope of $-5/3$. Two estimates were calculated for wave number ranges between 1-10cpm and 10-80cpm (Figure 13). The equation for the vertical (cross-stream) spectrum, $S_w(k)$, from McPhee 2008, is manipulated in order to solve for ϵ .

$$S_w(k) = \frac{4}{3} \alpha \frac{\epsilon^{\frac{2}{3}}}{k^{\frac{5}{3}}} \quad (3)$$

The $4/3$ constant comes from theoretical assumption of homogeneity in isotropic turbulence (Batchelor 1967). Alpha, α , is the Kolmogorov constant for the along-stream spectrum and has a value of .51 when k is the angular wave number in cycles per meter.

b. Chi

Analogously to ϵ , χ is defined as the rate of destruction of thermal variance in the water. The definition for χ was formulated by interpreting the molecular diffusion term in the temperature equation after multiplying through by another factor of T resulting in a term equal to:

$$\chi = K_T \left(\frac{\partial T}{\partial Z} \right)^2 \quad (4)$$

where K_T is the turbulent thermal diffusivity of seawater. From the diffusive term, χ can be defined as the rate at which temperature fluctuations are smeared away by molecular diffusion.

For this thesis, the microconductivity instruments determined χ 's numerical value by directly resolving the dissipation range of temperature. Dillon and Caldwell 1980 describe χ as the temperature variance dissipation rate satisfying:

$$\chi = 6 \times D \times \Omega^2 \times S_{cc_F} \quad (5)$$

where the constant 6 is due to the assumption of isotropy. D is the molecular diffusivity of seawater, 1.4×10^{-7} . Ω squared is the multiplication factor for the pre-emphasis frequency used to electronically pre-emphasize the microconductivity timeseries to form the gradient spectrum. And, the final term in the equation, S_{cc} , is the variance of the thermal microstructure gradient spectrum that resolves beyond the dissipation scale (Figure 14).

c. Turbulent Thermal Diffusivity

The turbulent thermal diffusivity, K_T , is effective diffusivity used to represent turbulent transport in circulation models that cannot resolve turbulent mixing eddies. It can simply be defined by manipulating equation (4) to say turbulent thermal diffusivity is equal to χ over the local background temperature gradient squared:

$$K_T = \frac{\chi}{(dT/dZ)^2} \quad (6)$$

The local vertical temperature gradient was calculated for each bottom-tracking segment over a 6m vertical scale. A Matlab script was written to first locate each of the bottom tracking segments and then the average was taken of the two profiles before and after each segment (Figure 15). Once the averages were obtained, the four gradients were then averaged together in order to estimate the temperature gradient for each bottom segment.

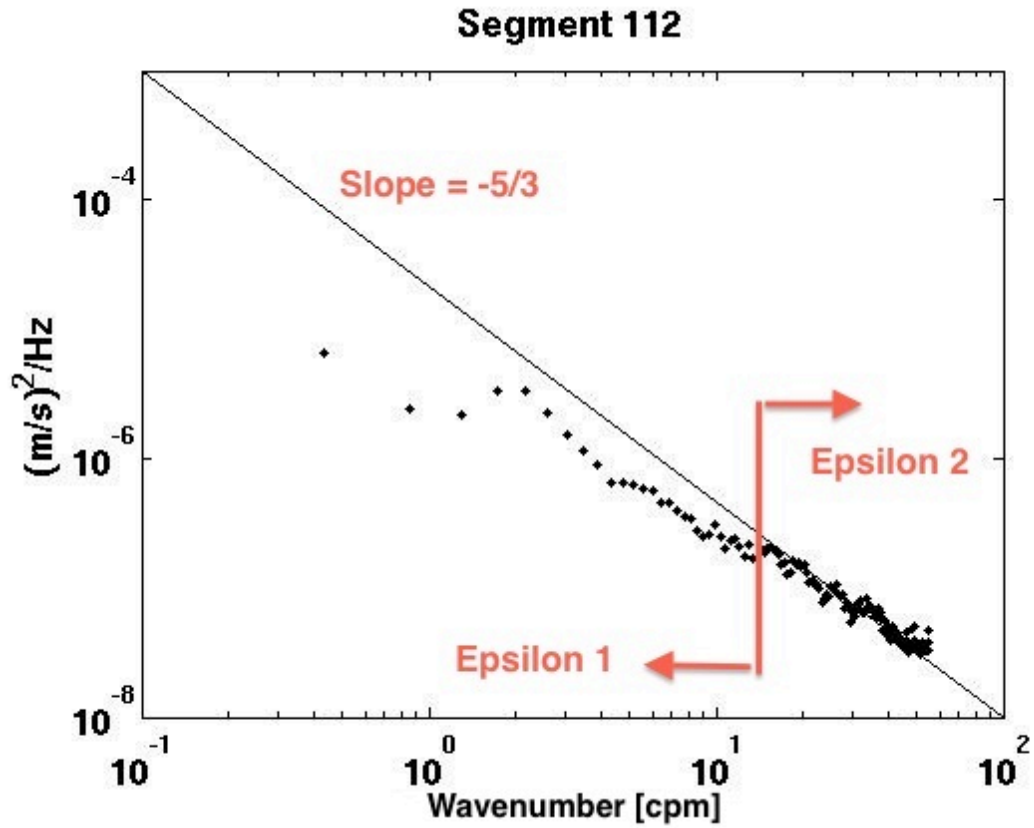


Figure 13. Amplification of the inertial sub range transfer scales. The line from the top left to the bottom right represents a $-5/3$ slope. Large-scale values are represented by epsilon 1 and small-scale values are represented by epsilon 2.

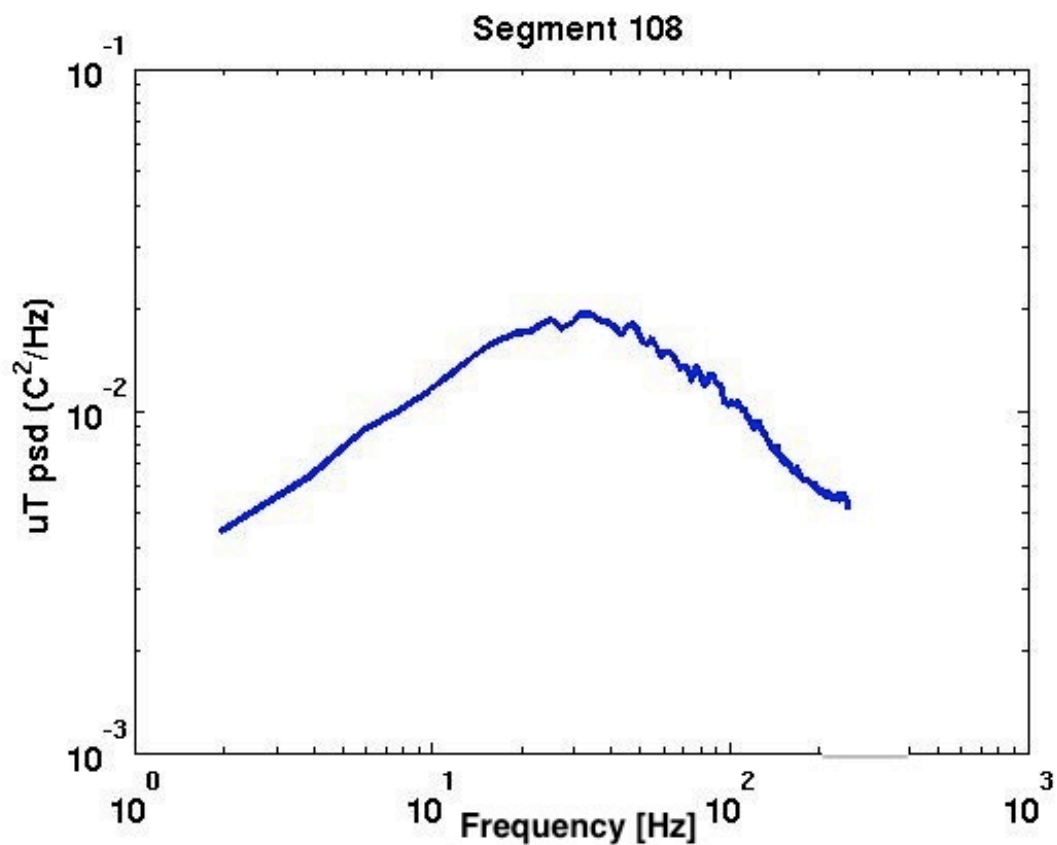


Figure 14. Thermal microstructure gradient spectrum calculated by the microconductivity instruments on board Daphne. The variance of this curve resolves beyond the dissipation rate for chi calculations.

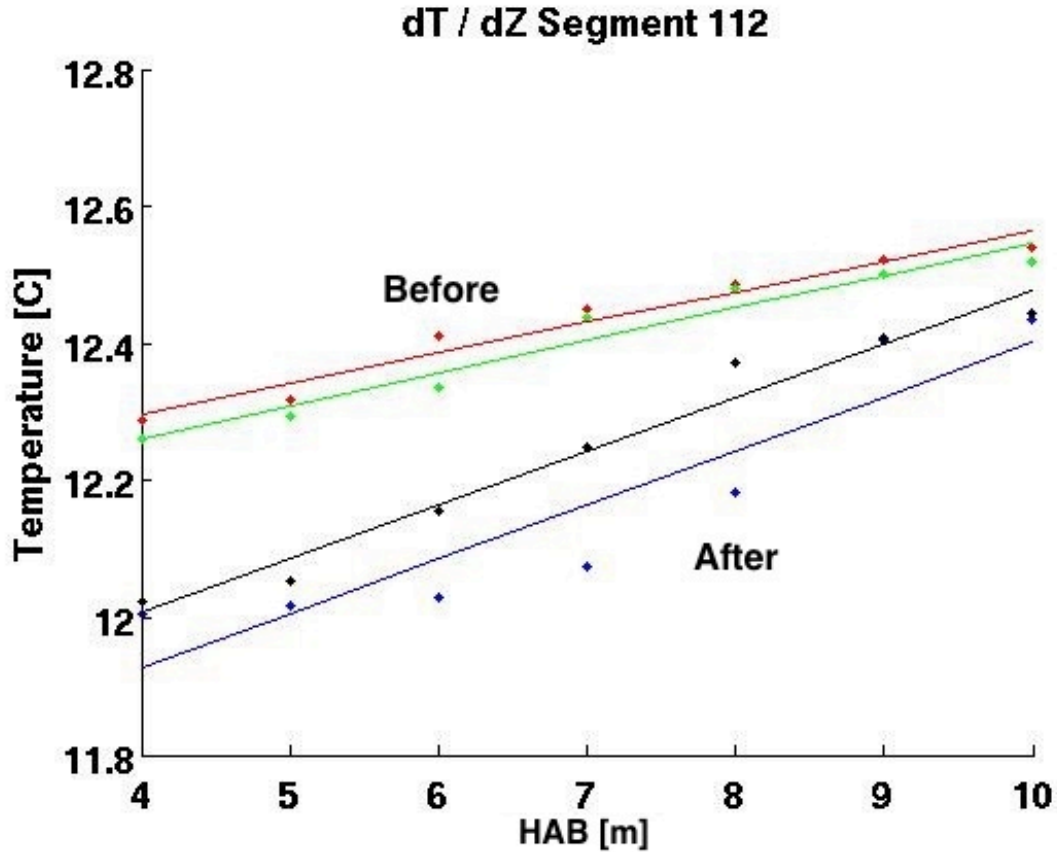


Figure 15. The local vertical temperature gradients of the four segments surround the bottom-tracking segment. Segment 112 is the bottom-tracking segment and is given a value of the mean to the four gradients averaged together.

B. BBL FRAME PROCESSING

1. ADCP

On the 21st of OCT, the frame was recovered from the experimental site. The data from the two ADCP instruments on the frame was extracted and processed in Matlab. These high-resolution instruments calculated velocity observations, specifically the U and V components, at the 60m-depth med-shelf location. After separating the two components of velocity, current speed was computed by summing the square of each velocity component and then taking the square root. Vertical shear was calculated by taking the vector vertical differential of the current. Acoustic backscatter was computed using the sonar equation:

$$EI = SL + SV + Con - 20\log(R) - 2\alpha R \quad (5)$$

where EI is the echo intensity in (dB). SL is the source level or transmitted power (dB). SV is the water-mass volume backscattering strength (dB). Alpha, α , is the absorption coefficient (dB/meter) and has a calculated value of .51 for the 300KHz ADCP and 2.1 for the 1200KHz ADCP. And R is the distance from the transducer to the depth cell (m). The constant, Con, is included because the measurement is relative rather than absolute. Each step along the process can be shown in a time series with a color intensity plot in Matlab to show both the current and acoustic backscatter profile timeseries for visual analysis of the water movement structure (Figure 16–17).

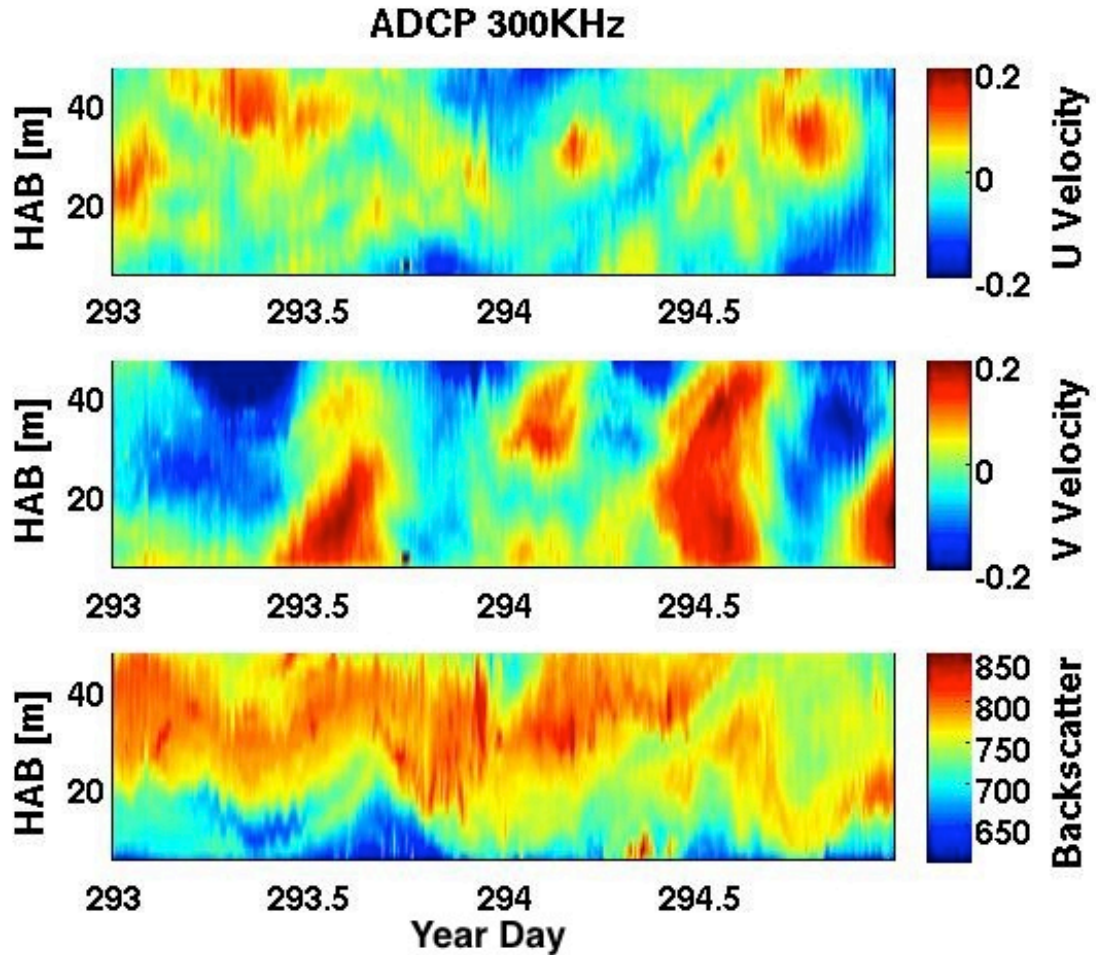


Figure 16. (Top panel) The cross-shelf or U component of velocity of the BBL frame. East is represented by the positive values in red and West is negative and in blue. (Middle panel) The along-shore (N or S) or V component of velocity.

North is positive and red and south is negative and blue. (Bottom panel)
 Calculated backscatter using the sonar equation.

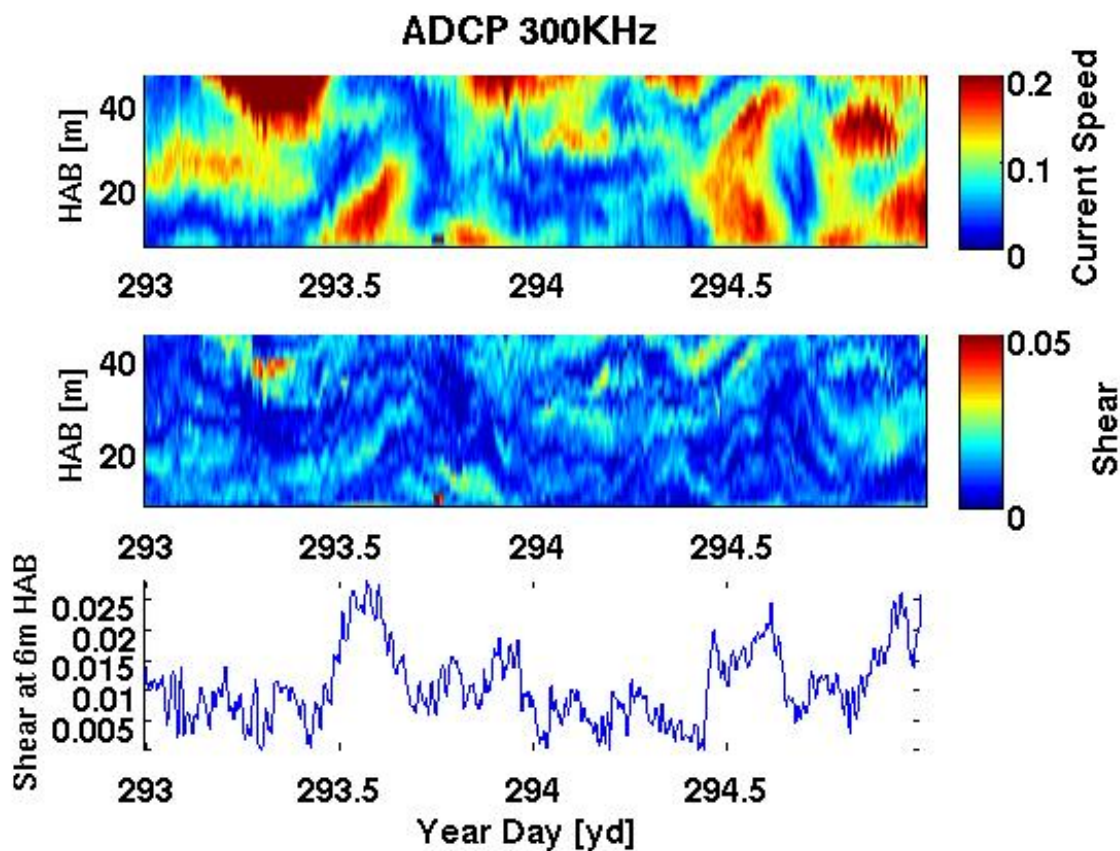


Figure 17. (Top panel) Current speeds in meters per second with red representing max speed and blue represents still water. (Middle panel) Vector differential of current represented by shear. (Bottom panel) Time series of shear at 6m HAB.

IV. RESULTS

A. SEDIMENT SUSPENSION

With an extensive amount of data collected during the NSF project in OCT 2012 by the BBL frame and the LRAUV, the first objective was to look at temporal and spatial views of the water column for the concentration of suspended, near-bed material and its relation to water column velocities. The ten-day span, YD 285 – 295, when the Daphne and Frame were both collecting data was the initial focus for analysis. Throughout the data analysis process for this time period it was important to keep track of where the LRAUV was in reference to the frame while it transected the continental shelf. Daphne was determined to be closest to the frame when it was 5m off the coast.

There were many different ways to represent turbidity in the BBL. For this discussion, the best attempt to confirm the presence of sediment suspension was to analyze a time series of a combination of instruments from both platforms. These instruments included the temperature and 650nm OBS on the LRAUV along with the frame's 1200KHz ADCP. Three of Daphne's onshore full profile transits spanning most of YD 293 were chosen. The onshore profiles were analyzed instead of the offshore near-bed profiles in order to get a broader view of the entire water column. A temperature time series of the water column is visually important to attempt to relate the stratification levels observed to the presence of turbidity in the water column. Optical measurements from Daphne will generate a spatial view of any benthic material present in the water column. The backscatter calculated from the 1200KHz ADCP on the frame is used in comparison with the OBS instrument on Daphne to amplify any benthic material near the bed as it passes over the frame. The 1200KHz ADCP was used over the 300KHz because the higher frequency will resolve benthic material better closer to the bed.

1. YD 293.04 – 293.12 of Sediment Suspension Event

While spatially tracking the particulate signature during YD 293.04-293.12 Daphne captures a great example of an internal nepheloid layer in figure 18, panel 2. In this panel, the turbidity seen by Daphne as it travels through the water column is

highlighted. A particularly high concentration of BBL turbidity is located around the 60m-depth range. At this depth, it is clear that the sediment spreads out laterally into the interior water column and into deeper water. The sediment remains suspended at its original depth level and temperature while propagating off shore, indicating the generation of an INL. Another area depicted having high turbidity levels is near the coast (right side of the panel) toward the top of the water column. It is speculated that this high concentration area is due to high levels of phytoplankton in the water column.

Panel 1 of figure 18 shows the temperature of the water column as Daphne transits onshore. By visual examination, the temperatures across the shelf would suggest high stratification levels. There is a well-defined two-layered thermal system present throughout the water column. The warmest water is concentrated at the surface of the water column and is separated from lower depths by a sharp thermocline. An upwelling of relatively cold water onto the mid and inner shelf appears to be necessary to allow the internal tidal bores to propagate onshore and create internal nepheloid layers.

The backscatter plot in panel 3 represents the turbidity seen near the seafloor by the 1200KHz ADCP of the frame. The ADCP observes high levels of turbidity throughout the first four meters of the water column. Highest turbidity levels are observed between YD 293.08-293.09 reaching about 6m HAB. These levels of turbidity support the quantities observed by the LRAUV as it passed the frame. Keeping in mind where the frame is located in reference to the LRAUV, a black line on panels one and two was inserted to represent the positioning of the frame, 5m offshore.

2. YD 293.44 – 293.53 of Sediment Suspension Event

A few hours after the first offshore transit, Daphne began its second near bed observation of the day. The first panel on figure 19 shows the stratification in the water column has remained close to the same from the transit earlier in the day. Cold isotherms (10 and 11C) have moved upwards and onshore close to the seabed. No relevant change was observed to the warmer water that was close to the surface of the water column.

Noteworthy changes have occurred in the OBS instrument on Daphne, panel 2, since the earlier transit. The INL has spread up the continental shelf into shallower

waters and the turbidity has become stronger. As a result, higher levels of turbidity are observed near the BBL closer to shore. At a distance of 4km off shore there is a clear formation of a nepheloid layer. Turbidity levels were found elevated in the water column about three orders of magnitude greater than the values of the first transit. Hypothesized phytoplankton levels near the surface at the coastline have slightly increased from earlier in the day.

Early reported levels during the time series of the backscatter show little to no turbidity present in the BBL, panel 3. As the day progresses, a peak in near-bed turbidity passes over the frame's ADCP where a steep increase is reported in suspended sediment. The well-observed turbidity region spread as high as the 7m HAB. The peak in turbidity correlates with the large-scale internal motions seen in the LRAUV section at 4km offshore. During the remainder of the section, turbidity levels began to decrease but at a much slower rate than they appeared.

3. YD 293.89 – 293.98 of Sediment Suspension Event

During the final transit of YD 293, panel 1 of Figure 20 shows the warmer waters have spread deeper into the water column, resulting in the colder isotherms near the bed being pushed offshore. As a result, stratification levels are lower than previously observed during the first two transits. Additionally, the distinctive two-layered system has become less definite.

Turbidity, panel 2, over the shelf is highest just off shore in no more than 40m of water. Over the rest of the shelf, sediment suspension is still observed but at depths much closer to the sea floor. There are no distinct INLs observed in the spatial view of the water column during this section. The backscatter plot supports the LRAUV optics recordings of small amounts of turbidity found near the seabed. Sediment suspension over the frame is only observed in the first 2m HAB.

4. Velocity and Shear during Sediment Suspension Event

To provide a context for the LRAUV transect profile and constant elevation sampling, the ADCP timeseries from the 60m deep fixed ADCPs has been analyzed.

Figure 21 is a time series of the ADCP profile timeseries results spanning from YD 292.5-294.5. The top two panels in the figure show the u and v components of velocity above the 300KHz ADCP. U velocity or cross-shore velocity describes the East (red/positive) and West (blue/negative) directions of currents. V velocity or along-shore velocity defines the North (red/positive) and South (blue/negative) currents. Both components experience directional changes to the water column over the two-day period. Around YD 293.5 a strong northerly flow with little cross-shore velocities was observed near the bed. The strong northerly flow was during the same time the INL present near the frame and indicates its direction of propagation. Near the bed a short time later, the along-shore velocity shifts to the south and the on shore velocity becomes dominated by westerly flow.

Current speeds are calculated by taking the absolute value of the u and v velocity components. By taking the vertical difference of the vector current profile, panel 4 was calculated and displays the shear magnitude in the water column. Shear is generated by the force of friction acting against the bed of the continental shelf. In order to better illustrate the near-bed shear experienced by the offshore LRAUV transits, a time series of the shear at 5m HAB was constructed in panel 5. The results from the shear at 5m HAB correlates well with the turbidity levels observed in the backscatter plot in panel 3 with the strongest shear observed between YD 293.5 and 293.9, the same time period as when the INL was present.

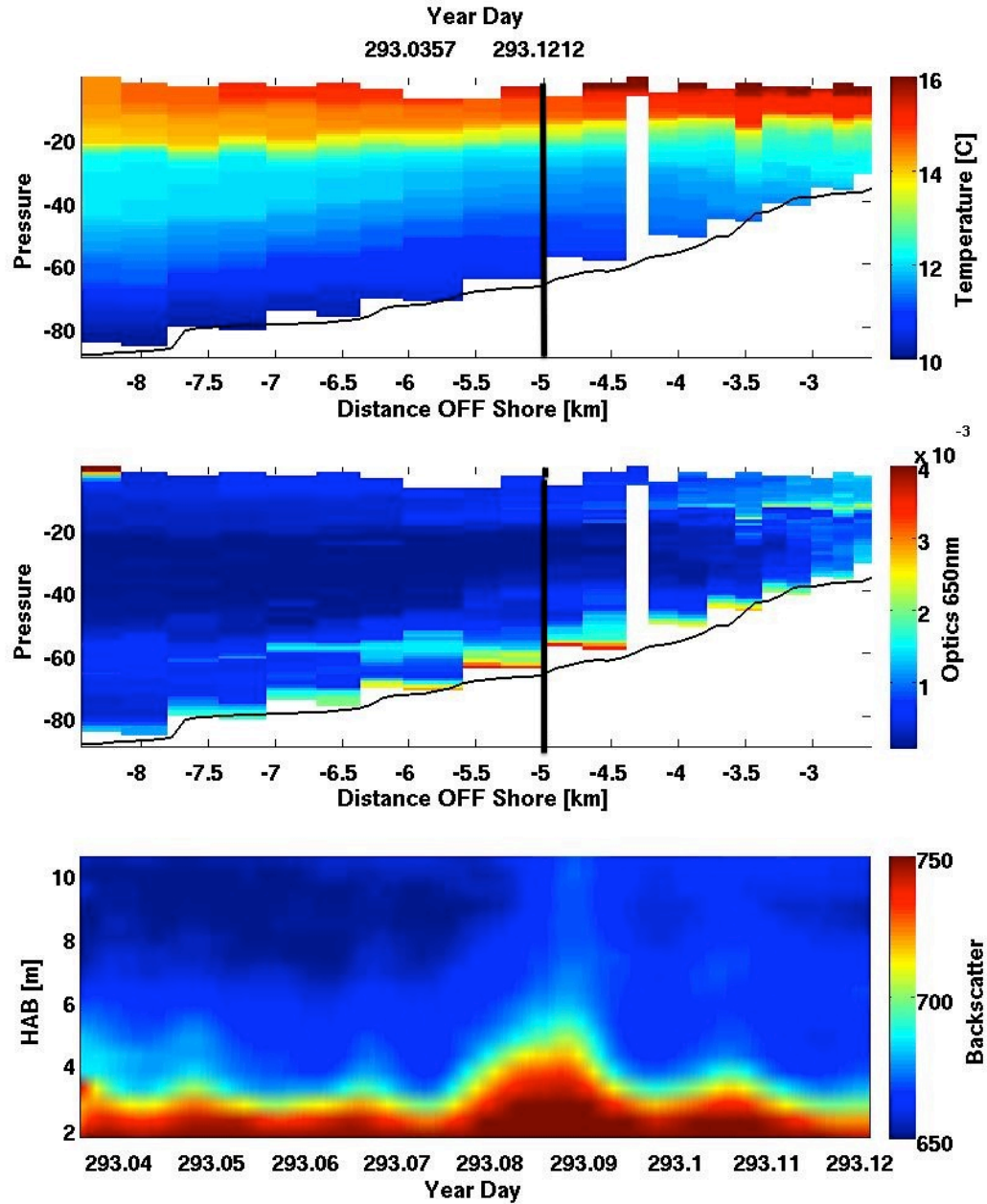


Figure 18. Suspended sediment event: YD 293.04 -293.12. Solid black vertical line represents the positioning of the frame as Daphne transits the shelf. The curved black line is the bathymetry of Monterey Bay. (Panel 1) Temperature of the water column as Daphne transits onshore. (Panel 2) Turbidity seen by Daphne as it propagates through the water column. (Panel 3) turbidity seen near the seafloor by the 1200KHz ADCP of the frame.

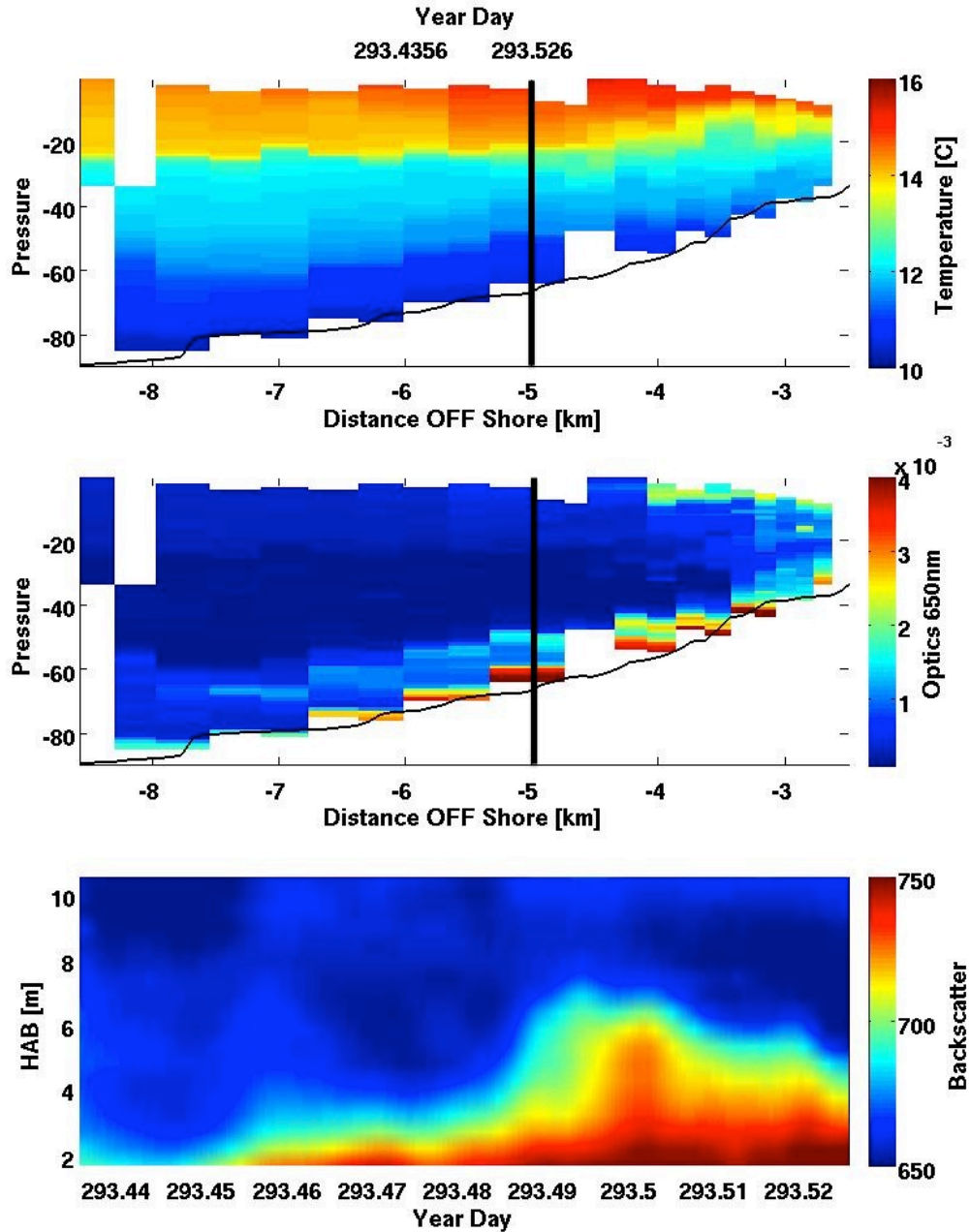


Figure 19. Suspended sediment event: YD 293.44-293.53. Solid black vertical line represents the positioning of the frame as Daphne transits the shelf. The curved black line is the bathymetry of Monterey Bay. (Panel 1) Temperature of the water column as Daphne transits onshore. (Panel 2) Turbidity seen by Daphne as it propagates through the water column. (Panel 3) turbidity seen near the seafloor by the 1200KHz ADCP of the frame.

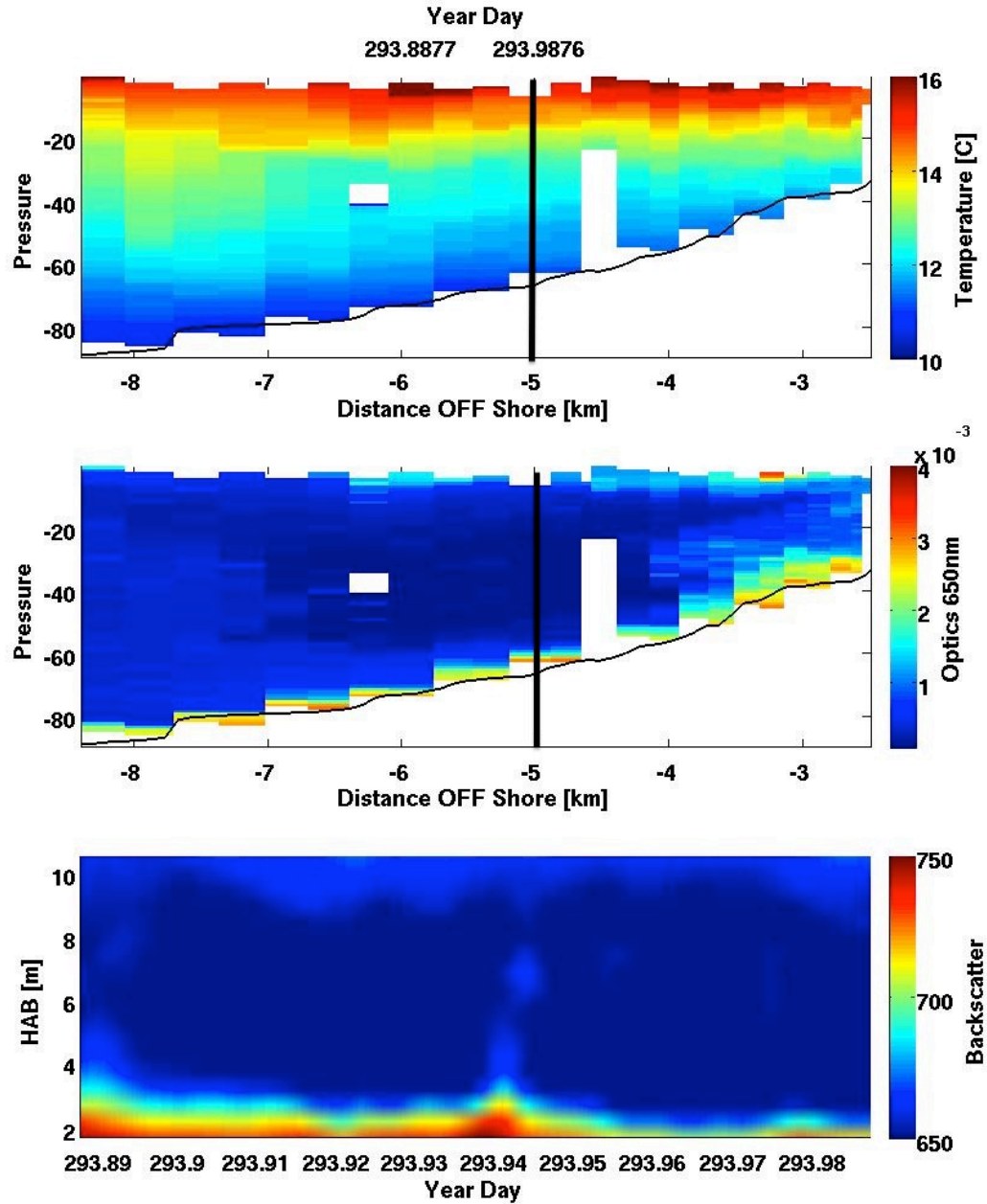


Figure 20. Suspended sediment event: YD 293.89-293.98. Solid black vertical line represents the positioning of the frame as Daphne transits the shelf. The curved black line is the bathymetry of Monterey Bay. (Panel 1) Temperature of the water column as Daphne transits onshore. (Panel 2) Turbidity seen by Daphne as it propagates through the water column. (Panel 3) turbidity seen near the seafloor by the 1200KHz ADCP of the frame.

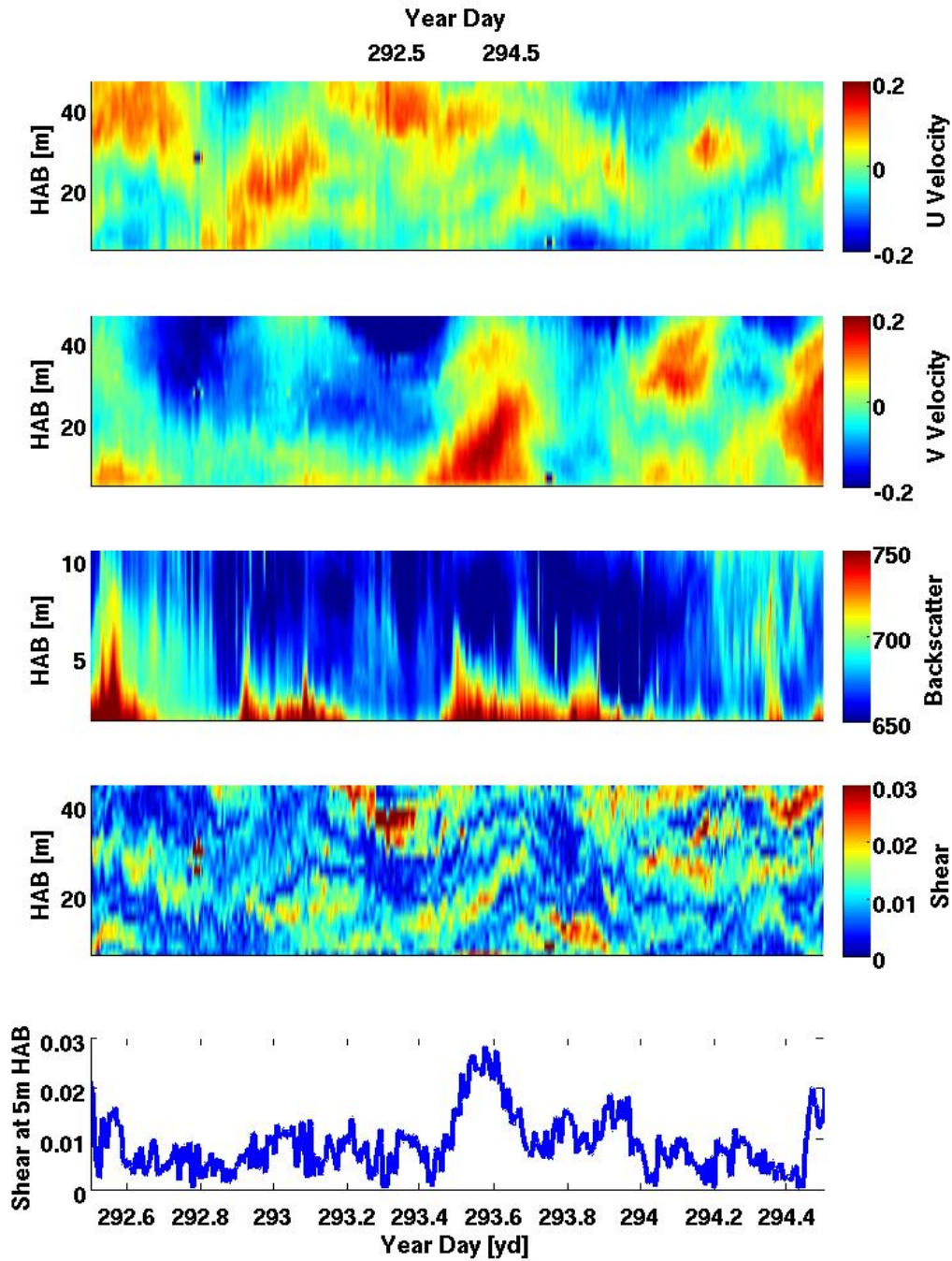


Figure 21. BBL Frame instruments covering sediment suspension event YD 293.04-293.98. (Panel 1 and 2) Velocity (u and v) magnitudes propagating over 300KHz ADCP. (Panel 3) Time series of backscatter from 1200KHz ADCP. (Panel 4) Shear values calculated from u and v velocity component of 300KHz ADCP. (Panel 5) Time series of calculated shear values at 5m HAB.

B. NEAR BED TURBULENCE

Previous research, in addition to the results from the previous chapter of this thesis, has shown the presence of INLs along the continental shelf of Monterey Bay. The answer to how these INL are generated has only been hypothesized in the past due to the complexity of these events. Motivation to understand how INL events are generated leads this analysis of the turbulence data collected from Daphne. Over the twenty days Daphne was collecting data, the turbulence instruments were recording high-resolution turbulence data. Only a subset of those twenty days had good microconductivity and ACM data for the sections after YD 302. In total, nine near bed sections between YD 302.1 and 303.77 provided useful turbulence data. Unfortunately, when the turbulence instruments were sampling the best data, the frame had already been recovered from the water; preventing analyses that could be made in conjunction with ADCP timeseries. In this particular analysis, the offshore sections of the LRAUV became the focal point for results. Offshore sections were examined by calculating the turbulence parameters for the bottom tracking segments.

In order to best describe internal tidal bores and solitons over the Monterey Bay Shelf, the offshore transit data from the LRAUV was broken down into multiple six-panel figures. The panels consist of the LRAUV height above bed, temperature, OBS, and the three turbulence calculations: ε , χ , and K_T . In addition, for all bottom-tracking segments, the thermal gradient spectra were calculated from the microconductivity sensor. For this discussion, ITB events were classified into two distinct subgroups: bore events or bore events with solitons.

1. Internal Tidal Bore Event

Figure 22 spans YD 303.28-303.36 and is characterized as an internal tidal bore event. Such classifications can be made by first analyzing the ε values, panel 3, for turbulence levels. Between YD 303.29 and 303.32, the near bed segments of section 76, highlighted in blue, green, red, and cyan, show exceptionally high turbulence values, indicating the passing of an ITB. After observing high turbulence near the bed, it is important to then examine the temperature gradients, panel 2. There is not much of a

temperature gradient observed during these segments and are fairly consistent, therefore confirming that no solitons are present. OBS calculations, panel 3, show quite high sediment suspension along the bed throughout the entire transit offshore. Even after the turbulence has subsided, indicated by lower ε values, the turbidity near the sea floor remains.

The thermal gradient spectra are presented in Figure 23. As expected, the observed segments with high turbulence have much higher thermal gradient spectral levels than those with low ε values. The spectral peak and rapid roll-off at higher frequencies for turbulence is consistent with the Batchelor spectrum, and is evidence of high-quality turbulence data.

2. Soliton Events

With some of the high-energy ITB events, packets of solitons on the leading edge of the bore can be seen. These particular events had a significant impact on the water column structure as the LRAUV “flew” through them. An ITB with a soliton on the leading edge is an extremely nonlinear baroclinic process. Isotherm displacements and increased turbulence levels that change suddenly, rather than sinusoidal oscillations, indicate the nonlinear baroclinic process.

An example of the presence of a soliton is seen during section 64 (Figure 24). By examining each near bed segment, the pulse-like changes in temperature at 5m HAB indicate the presence of a train of solitons followed by the ITB. During the first segment (blue) the water column is fairly quiet, with no isotherm displacement, turbidity, or turbulence detected. However, on the second segment (green) a very energetic soliton set passes through the BBL, indicated by oscillating isotherms. As a result, turbidity in the water column rises and falls with the pulse-like solitons. In addition to the increased turbidity, the BBL becomes much more turbulent. After the soliton on the leading edge of the ITB has passed, turbulence levels maintain a high value while the rest of the bore passes across the shelf.

Only a day after the first soliton was observed, Daphne measures a second one as it was conducting its near bed transits. The first segment of section 74 captures the highly energetic soliton. Large fluctuations in temperature were observed as the LRAUV

sampled 5m off the sea floor. Each time an isotherm displaced from warm to colder water, an increase in turbidity was observed. Similar to the first soliton event, turbulence levels were increased near the bed within the soliton, but the turbulence levels decreased after the soliton passed. Therefore, the thermal gradient spectrum only shows the first segment energetic with turbulence and the subsequent segment inactive.

Finally, during one of Daphne's final offshore transits, a third soliton event disturbed the water column (Figure 28). Large oscillations were observed in the temperature spatial sampling over the first two segments (blue and green). Depressions in the isotherm, increased turbidity, and increased turbulence were all observed during the same time along the transit. Following the soliton event, the turbulence levels in the water column varied between high and lower levels. The spectrum associated with the soliton event produce well-shaped Batchelor spectra that fall off at high frequencies.

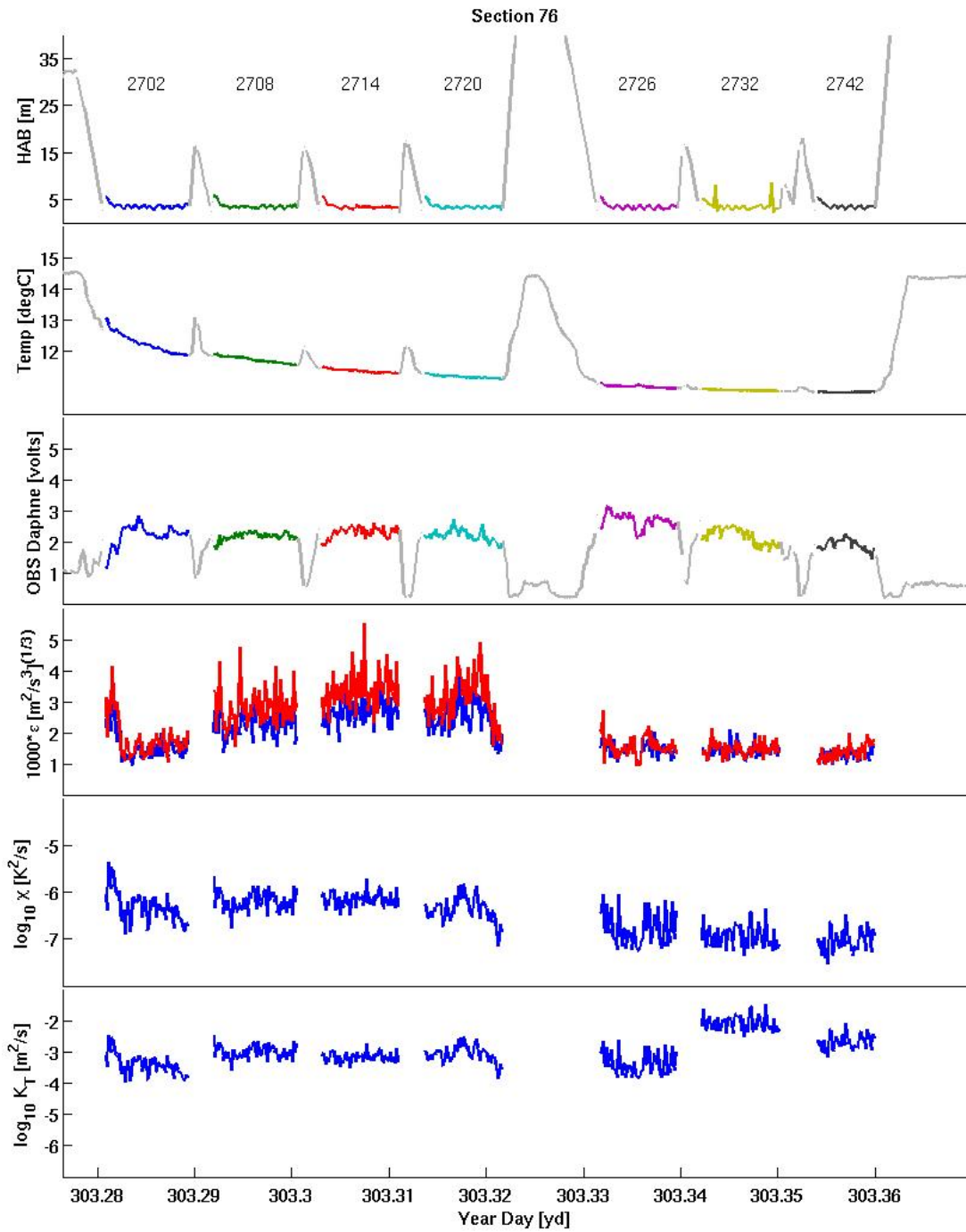


Figure 22. Offshore transit of Daphne section number 76. (Panel 1) Lateral view of the LRAUVs movements throughout the water column with segment numbers over the bottom tracking segments. (Panel 2) Temperature observed. (Panel 3) OBS from Daphne. (Panel 4-6) Turbulence calculations for epsilon, chi, and K_T

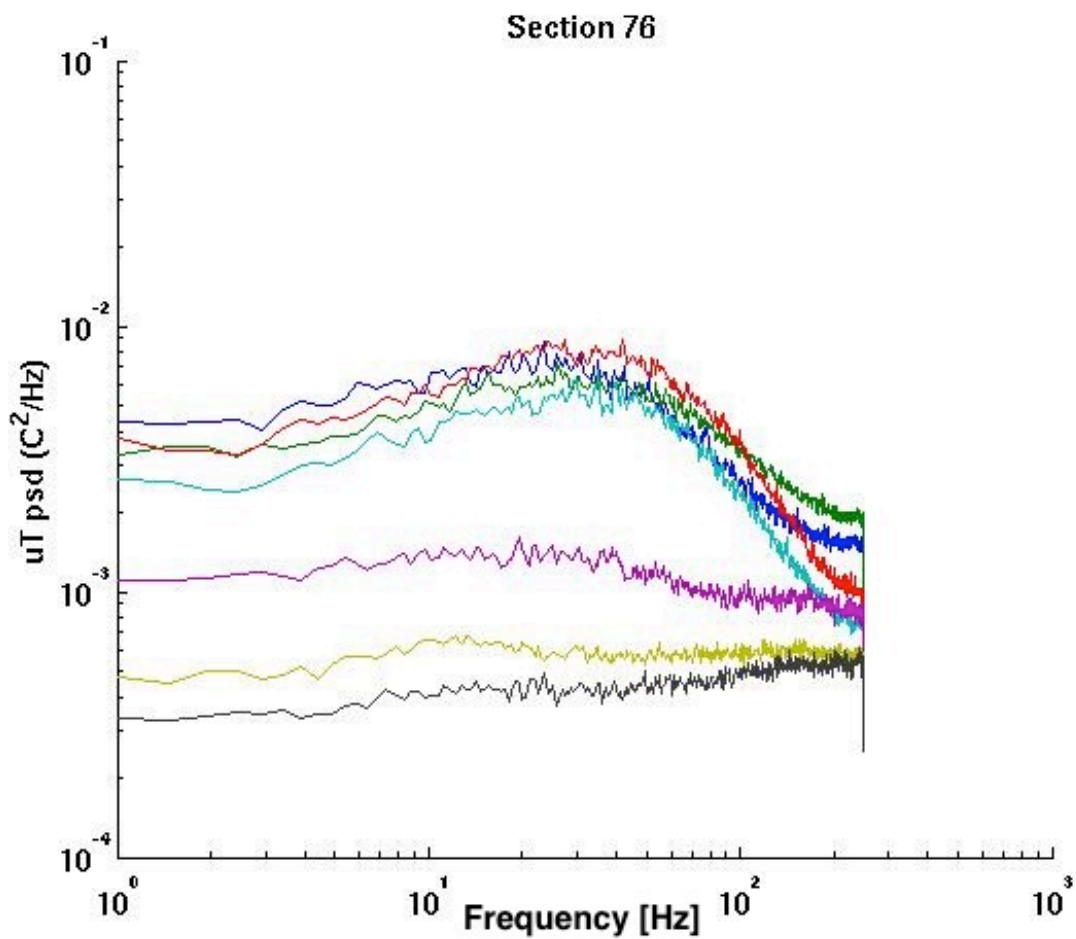


Figure 23. Thermal microstructure gradient spectrum calculated by the microconductivity instruments on board Daphne of each bottom-tracking segment over section number 76. Colors correlate with previous figure of the same offshore transit section.

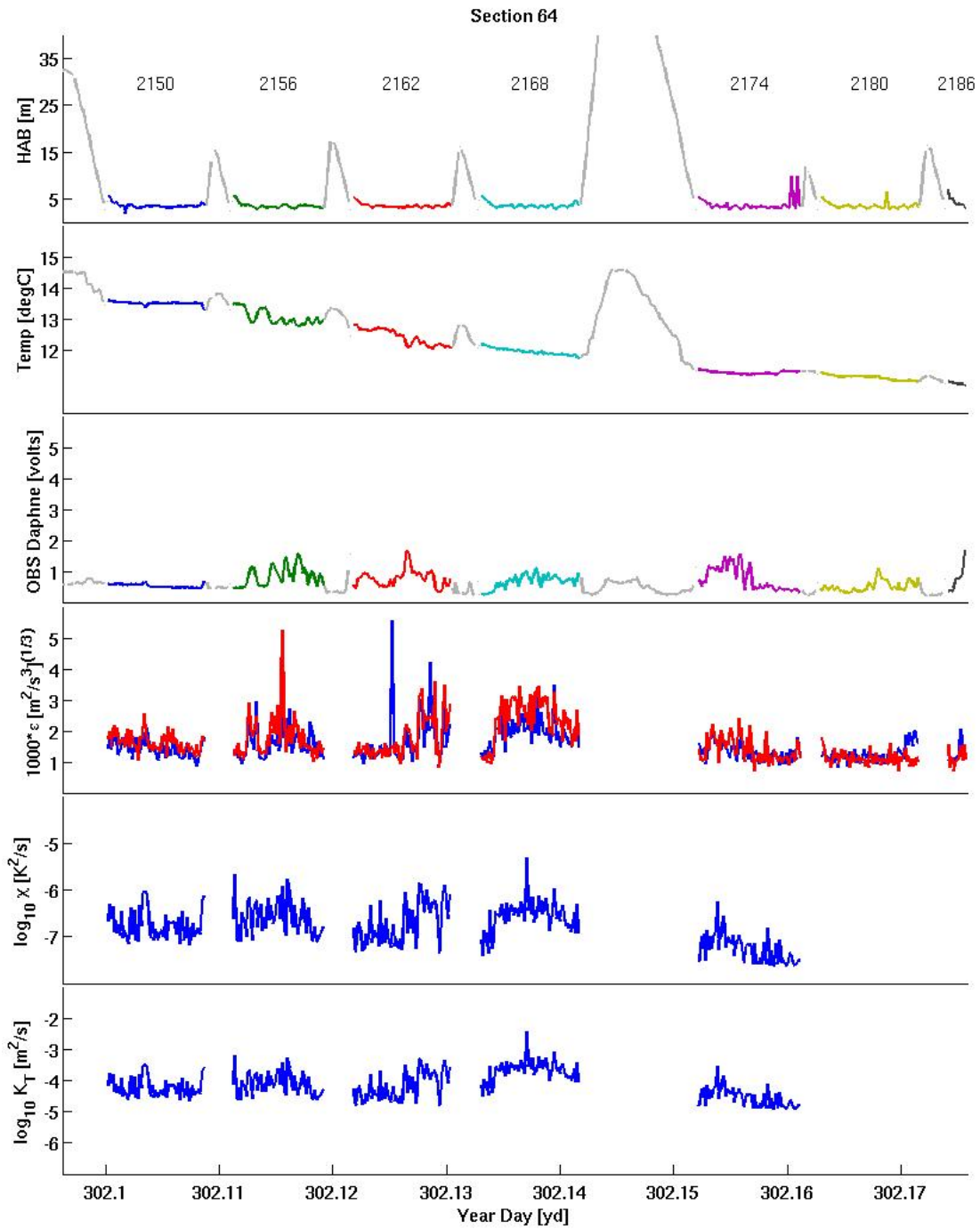


Figure 24. Offshore transit of Daphne section number 64. (Panel 1) Lateral view of the LRAUVs movements throughout the water column with segment numbers over the bottom tracking segments. (Panel 2) Temperature observed. (Panel 3) OBS from Daphne. (Panel 4-6) Turbulence calculations for epsilon, chi, and K_T

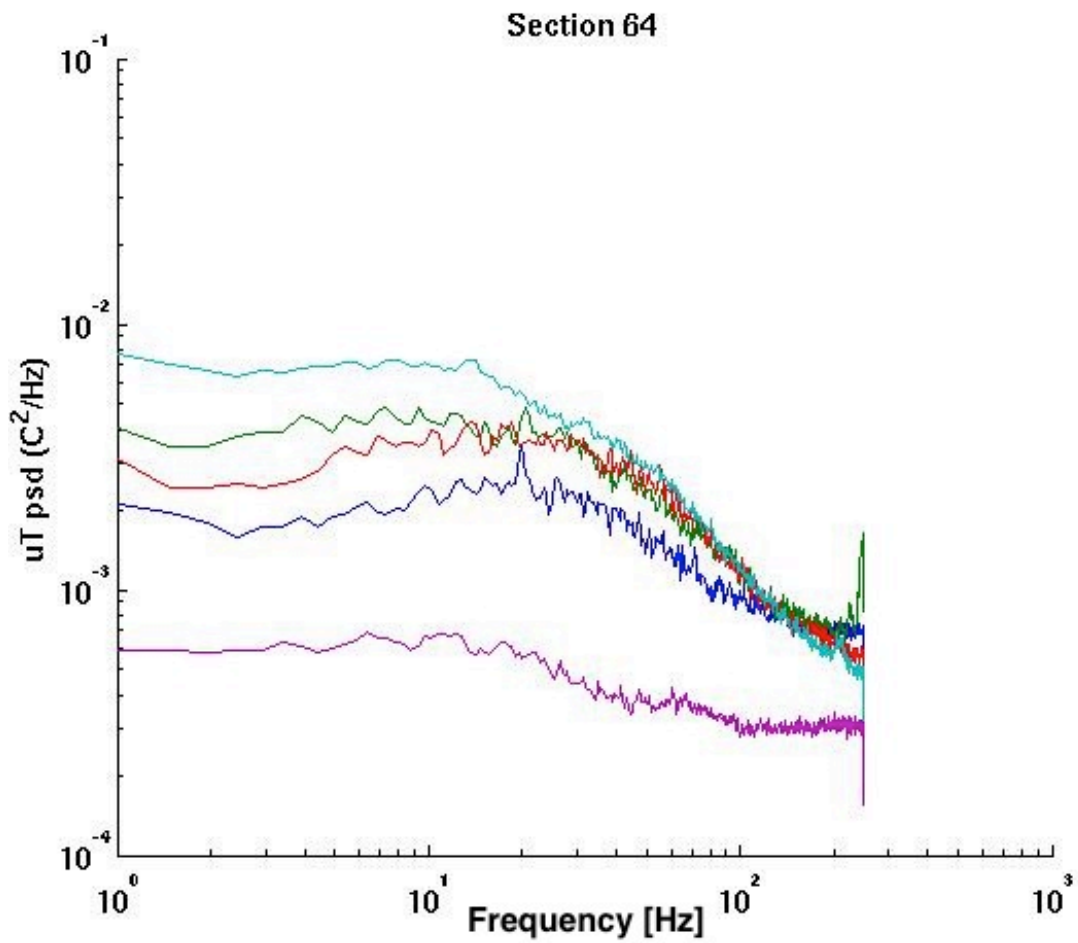


Figure 25. Thermal microstructure gradient spectrum calculated by the microconductivity instruments on board Daphne of each bottom-tracking segment over section number 64. Colors correlate with previous figure of the same offshore transit section.

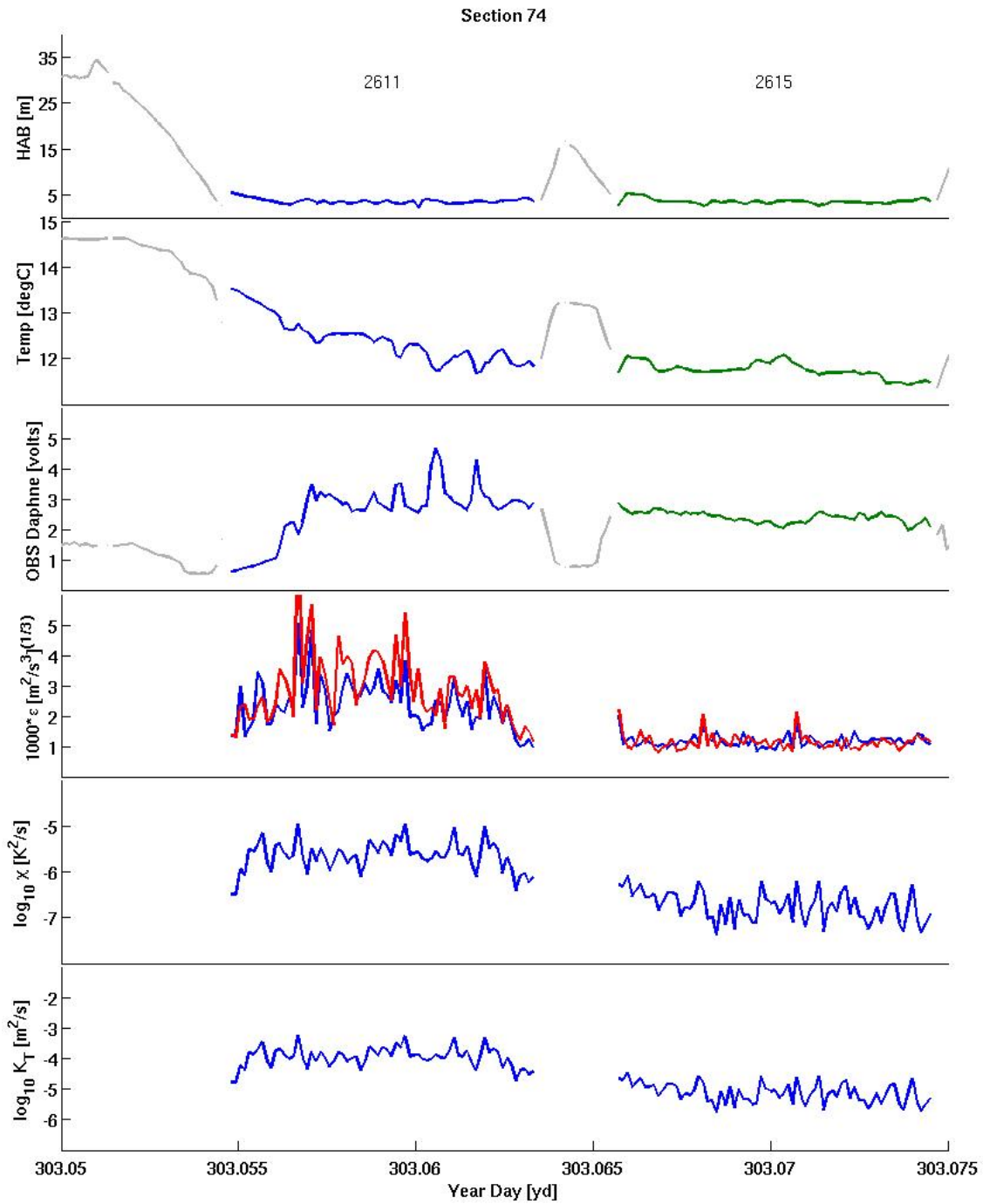


Figure 26. Offshore transit of Daphne section number 74. (Panel 1) Lateral view of the LRAUVs movements throughout the water column with segment numbers over the bottom tracking segments. (Panel 2) Temperature observed. (Panel 3) OBS from Daphne. (Panel 4-6) Turbulence calculations for epsilon, chi, and K_T

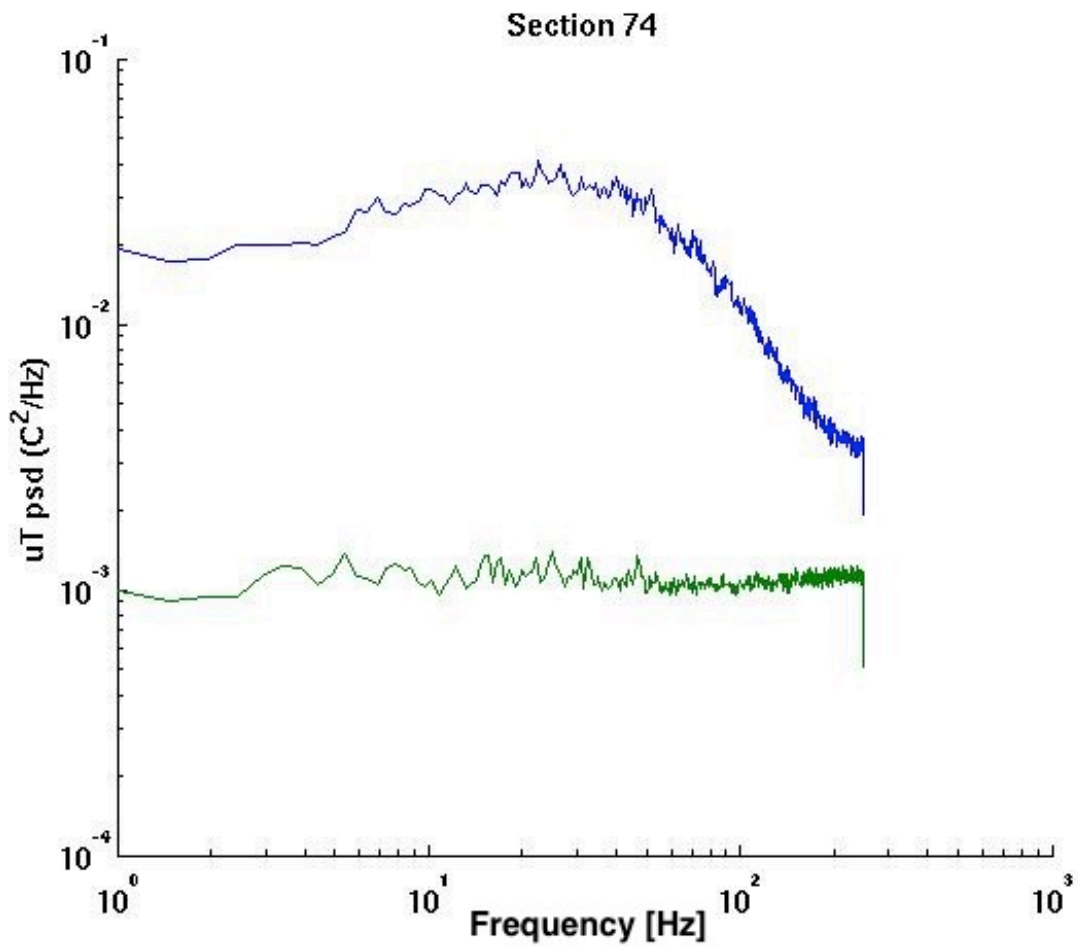


Figure 27. Thermal microstructure gradient spectrum calculated by the microconductivity instruments on board Daphne of each bottom-tracking segment over section number 76. Colors correlate with previous figure of the same offshore transit.

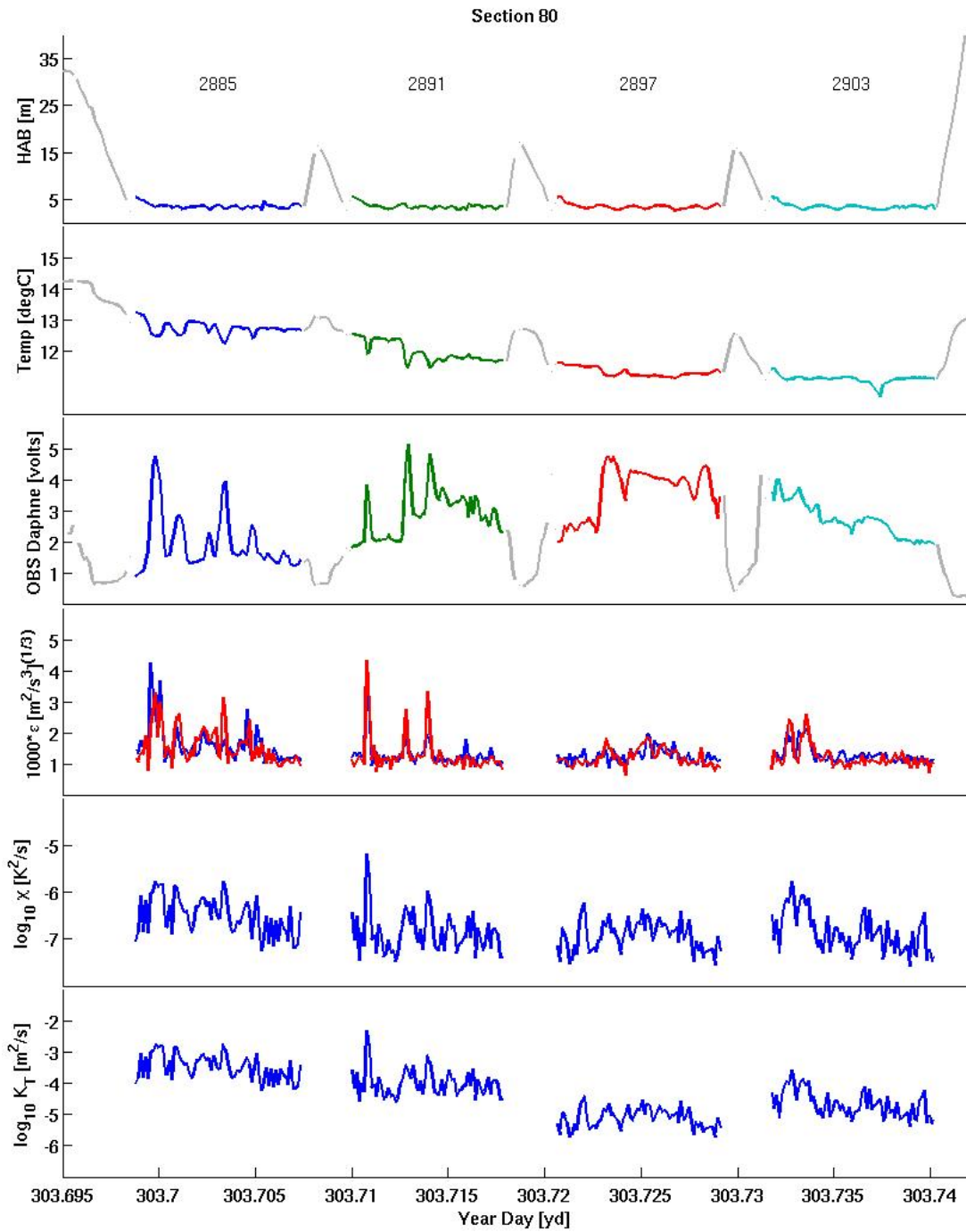


Figure 28. Offshore transit of Daphne section number 80. (Panel 1) Lateral view of the LRAUVs movements throughout the water column with segment numbers over the bottom tracking segments. (Panel 2) Temperature observed. (Panel 3) OBS from Daphne. (Panel 4-6) Turbulence calculations for epsilon, chi, and K_T

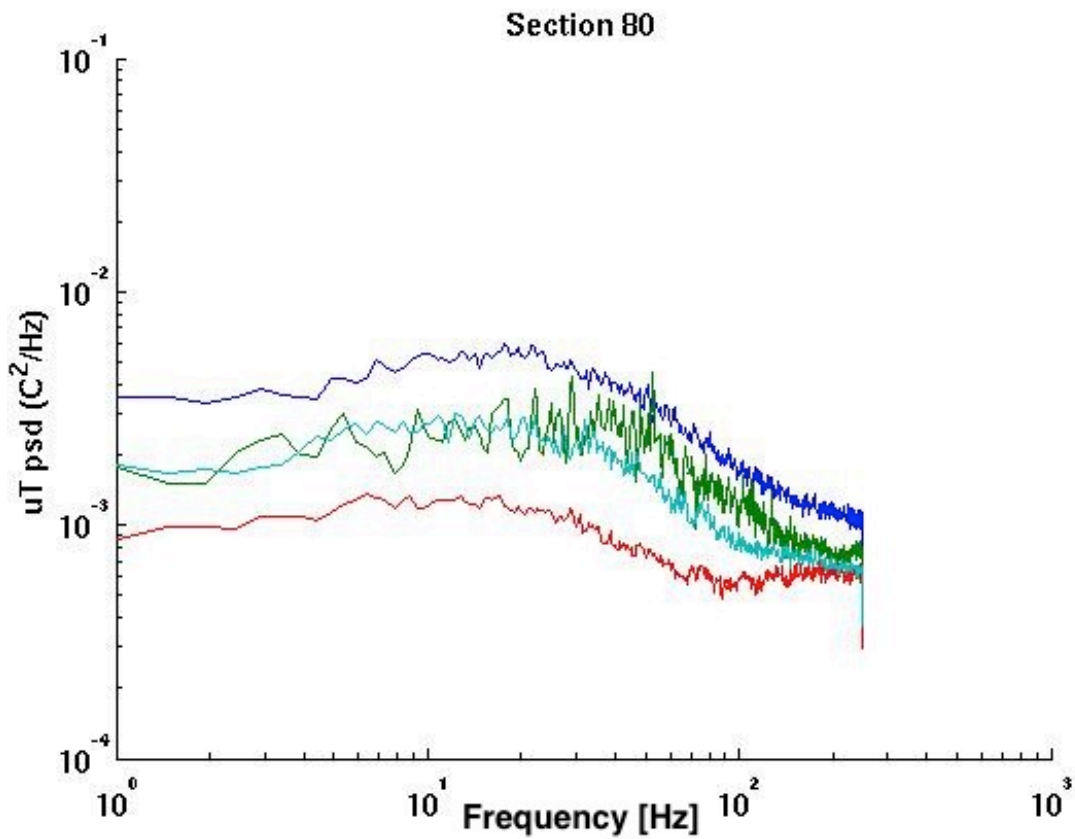


Figure 29. Thermal microstructure gradient spectrum calculated by the microconductivity instruments on board Daphne of each bottom-tracking segment over section number 80. Colors correlate with previous figure of the same offshore transit.

THIS PAGE INTENTIONALLY LEFT BLANK

V. DISCUSSION

A. SUSPENDED SEDIMENT EVENTS

Monterey Bay experiences high levels of near-surface stratification during late summer, approximating a two-layered system. Over the course of the NSF experiment, high-level stratification events were captured by the temperature profile transects measured by the LRAUV as it transited the water column. During the three transects by Daphne on YD 293 a transition from a strong two-layered stratification in the morning to a less defined and weaker stratification at night was observed. At this time cold isotherms were pushed onshore due to the effect of internal tides. Other researchers have shown how the processes of coastal upwelling, which raises the stratification levels, amplify this shifting in cold isotherms onshore.

As hypothesized, the origin of the INL was found to be between 60-70m depths and subsequently, the suspended sediment was observed to spread horizontally from the origin as far as 2.5km along the continental shelf. After suspension has occurred, the INL seems to propagate up the shelf. Support for shore ward propagation is found in the high concentrated levels of turbidity found near the shore at the end of YD 293.

By further analyzing the velocity measurements captured from the 300KHz ADCP, it can be determined that during YD 293 an ITB was propagating down from the north. During this time, large amounts of shear and turbidity were present near the sea floor and influenced the generation of the INL. In order to further explore how the INLs are created and propagate, turbulence levels were analyzed.

B. TURBULENCE EFFECTS

Internal tidal bores and solitons were frequently observed providing the necessary stress and turbulence levels near the bed to suspend sediment into the water column. During section 76, high levels of turbulence were observed without any presence of high frequency solitons at its leading edge. After the highly turbulent bore passed and increased the level of turbidity near the bed, the suspended sediment did not quickly return to the seabed. Therefore, turbidity caused by ITBs can remain in the water column

for multiple hours after the bore has passed. During active periods of internal tidal waves it is difficult to determine exactly how long the turbidity levels remain suspended because currents advected the INLs.

When solitons were observed around depth levels of the frame, section 64, they were closely followed by their accompanied ITB. The results for this section confirm that solitons are found on the leading edge of the ITB and propagate in strong unidirectional pulses of current over the shelf. During analysis of sections 74 and 80, high levels of turbulence did not follow the solitons but rather they were followed by a period of low turbulence. One explanation to why the ITB was not seen following the soliton can come from the detection location of the soliton on the shelf. After solitons have been generated at the leading edge of an ITB, they have the ability to break away and propagate at a much faster rate than the ITB. Therefore, when solitons are found close to the shoreline and followed by periods of calm turbulence, it can be speculated that these highly non-linear soliton pulses have propagated ahead of the ITB.

ITBs and solitons create enough turbulence within the BBL that high levels of turbidity are seen as they pass through. Surface wave forcing can help to suspend and entrain the sediment, but these observations suggest that the solitons and tidal bores are the dominant force for transport up into the water column and net transport of sediment. On the other hand, local high turbulence is not a necessary condition for high levels of suspended sediment to exist. For example, in figure 26, the second segment has low turbulence values but a rather high level of turbidity. Such events can occur in the water column because of advection and the relatively long settling time of the suspended sediment.

VI. CONCLUSION AND RECOMMENDATION

A. SUMMARY

The effects of shoaling inner shelf internal tidal bores and solitons on the bottom boundary layer have been observed and analyzed during October 2012 from Moss Landing to Monterey Bay in Monterey, CA. This research utilized measurements from two different observing systems: the long range propeller-driven AUV called Daphne, and a bottom boundary layer frame measuring changes in temperature, conductivity, pressure, optics, current profiles, and turbulence during a four week time period. The data collected from these platforms were used to capture the strength of the internal tides and their influence on the bottom boundary layer as they propagate and entrain sediment into the upper water column. Internal tidal bores and soliton velocities had components in both cross-shore and alongshore directions. Internal bore events may be categorized by whether or not they contained solitons. Due to the nonlinear nature of solitons, no consistent pattern, shape, duration, or maximum excursion could be linked between each event. However, each soliton train was characterized by their steep isotherm excursions. In addition, solitons, when present, are always found propagating in front of the bores, generated at the leading edge, but can separate away from the slower moving ITB.

The main focus for this field study, sponsored by the National Science Foundation, was to quantify turbulent stress levels for heightened events near the bed. In addition, link any possible correlations with turbulence and the generation of internal nepheloid layers. Typical ε values for high turbulent events were $1\text{e-}7 \text{ m}^2/\text{s}^3$, with turbidity levels near the bed increased on average by a third. During these events it was directly observed that fine bed sediment was transported upward into the entrained water column where they can form INLs. Observations show how strong changes in the water column currents, turbidity, and turbulence would have a large effect on divers and subsurface operating vehicles. Further research is required to provide a predictive capability of this variability.

B. NAVAL IMPACT

Results from this research are valuable in better understanding the highly complex coastal environment and how bathymetry such as submarine canyons and shelf breaks can generate tidal forced waves. Regions of strategic military interest, including the South China Sea and straits of Gibraltar, are frequently populated by ITB and soliton activity. Energetic internal disturbances like bores and solitons can disrupt and alter military operation missions. These missions include but are not limited to mine warfare, submarine warfare, and special operation warfare. Increased knowledge of the diverse coastal environment would result in improvements to littoral operations, nearshore model resolution, and a better understanding of the coastal acoustic environment.

C. RECOMMENDATIONS FOR FUTURE RESEARCH

Potential research suggestions from this fieldwork include analyzing the data from other instruments on the BBL frame. The BCDVSP is a non-invasive, high-resolution acoustic instrument that measures turbulent stress within internal waves and any low-frequency current boundary layers. By analyzing such data, turbulent vertical and lateral sediment fluxes can be estimated at centimeter resolutions. In addition, to the BCDVSP there were temperature sensors ever 2m up to 16m HAB attached to the cable connecting the frame to the surface buoy. The temperature sensors would aid in resolving any steep temperature gradients generated by internal tidal bores and solitons. Furthermore, the strength of ITB events could be further characterized by analyzing the wind and tide relationship with the currents over the continental shelf.

Future deployments would benefit from having both the BBL frame and the LRAUV operational in order to collect the necessary data to best capture these complex tidal events. Utilizing the array of instruments attached to the two platforms will produce enough necessary data to better categorize and explain the extremely nonlinear internal events better than ever done before. The implementation of the flux package to the front of the LRAUV provided excellent turbulence data and would benefit any future study of internal tidal bores and solitons. An increasing understanding of the effects that tidal bores have on the generation of INLs will strongly enhance the US Navy's dominance of the undersea domain. Ultimately, this understanding will provide the decision makers of the future the necessary knowledge to ensure optimal planning for costal naval missions.

LIST OF REFERENCES

- Apel, J.R., L.A. Ostrovsky, Y.A. Stephanyants, and J.F. Lynch, 2007: Internal solitons in the ocean and their effect on underwater sound, *J. Acoust. Soc. Am*, **121**, 695–722.
- Baines, P.G., 1982: On internal tide generation models, *Deep Sea Research*, **29**, 3A, 307–338.
- Batchelor, G.K., 1967: *The Theory of Homogeneous Turbulence*, Cambridge University Press, Cambridge.
- Carter, G.S., M.C. Gregg, R.C. Lien, 2005: Internal waves, solitary-like waves, and mixing on the Monterey Bay shelf. *Continental Shelf Research*, **25**, 1499–1520.
- Cazenave, Francois, Y. Zhang, E.E. Mcphee-Shaw, J.G. Bellingham, and T.P. Stanton, 2011: High-resolution surveys of internal tidal waves in Monterey Bay, California, using an autonomous underwater vehicle. *Limnol. Oceanogr.*, **9**, 571– 581.
- Crabbe K.L., 2007: Directional characteristics of inner shelf internal tides M.S. thesis, Dept. of Oceanographic Studies, Naval Postgraduate School, 94.
- Department of the Navy, cited Nov 9, 2012: The Navy Unmanned Undersea Vehicle (UUV Master Plan) [Available online at <http://www.dtic.mil/cgibin/GetTRDoc?AD=ADA511748&Location=U2&doc=GetTRDoc.pdf>]
- Farmer, D.M., and L. Armi, 1999: The generation and trapping of internal solitary waves over topography. *Science*, **283**(5398), 188–190.
- Foreman, M.G.G., 1995: Tide removal requiring a dynamical interpretation. *Quantitative Skill Assessment for Coastal Ocean Models*, D.R. Lynch and A.M. Davies, Eds., Amer. Geophys. Union, 224–239.
- Garrett, C., 2003: Ocean science: Internal tides and ocean mixing, *Science Week*, **301**, 1858–1859.
- Gordon, Lee, 1996: Acoustic Doppler Current Profilers, Principles of Operation: A Practical Primer. *RD Instruments*, 33–43.
- Hickey, B.M., 1998: Coastal oceanography of western North America from the tip of Baja California to Vancouver Island, *The Sea*, **11**, 345–393.

- Holloway, P.E., 1987: Internal hydraulic jumps and solitons at a shelf break region on the Australian North West shelf. *J. Geophys. Ocean.*, **92**, 5405–5416.
- Huthnance, J.M., 1989: Internal tides and waves near the continental shelf edge. *Geophys. Astrophys. Fluid Dyn.*, **48**, 81–106.
- Johnston, T. M. S., D. L. Rudnick, G. S. Carter, R. E. Todd, and S. T. Cole, 2011: Internal tidal beams and mixing near Monterey Bay, *J. Geophys. Res.*, **116**, C03017, doi:10.1029/2010JC006592.
- Kantha, L.H., and C.A. Clayson, 2000: Small scale processes in geophysical fluid flows. Academic Press, San Diego, CA.
- McManus, M., R. Kudela, M. Silver, G. Steward, P. Donaghay, and J. Sullivan, 2007: Cryptic blooms: Are thin layers the missing connection? *Estuaries and Coasts*, doi10.1007/s12237-007-9025-4.
- McPhee, M. 2008: Air-ice-ocean interaction: turbulent ocean boundary layer exchange processes. McPhee Research Company, Naches, WA.
- McPhee-Shaw, E.E. 2002: Boundary layer intrusions from a sloping bottom: A mechanism for generating intermediate nepheloid layers, *J. Geophys. Res.*, **107**, C6 doi 10.1029/2001/JC0000801.
- McPhee-Shaw, E.E., R.W. Sternburg, B. Mullenbach, and A.S. Ogston, 2004: Observations of intermediate nepheloid layers on the northern California margin. *Continental Shelf Research*, **24**, 693–720.
- McPhee-Shaw, E.E., D. Siegel, L. Washburn, M. Brzezinski, J. Jonesm A. Leydecker, and M. Melack, 2007: Mechanisms for nutrient delivery to the inner shelf: Observations from Santa Barbara Channel, *Limnol. Ocenogr.* **52**, 1748–1766.
- Monterey Bay Aquarium research, cited 2013: LRAUV detailed description. [Available online at <http://www.mbari.org/default.htm>]
- National Centers for Coastal Ocean Science, cited Jan, 2013: Ecosystems [Available online at <http://www.cop.noaa.gov/ecosystems/>].
- Nelson, W.G. et al., 2008: Ecological Condition of Coastal Ocean Waters along the U.S. Western Continental Shelf: 2003, *NOAA Technical Memorandum NOS NCCOS 79*, EPA 620/R-08/001. 137 p.
- Nobel, M.A., B. Jones, P. Hamilton, J.P. XU, G. Robertson, L. Rosenfeld, and J. Largier, 2009: Cross-shelf transport into nearshore waters due to shoaling internal tides in San Pedro Bay, CA. *Continental Shelf Res.*, doi:10.1016/j.csr.2009.04.008.

- Ostrovsky, L.A., and Yu. A. Stepanyants, 1989: Do internal solitons exist in the ocean?. *Revs. Geophys.*, **27**, 293–310.
- Partnership for Interdisciplinary Studies of Coastal Oceans, cited Jan, 2013: Coastal Oceans [Available online at <http://www.piscoweb.org/research/coastal-oceans>].
- Patti, B., C. Guisande, A.R. Vergara, I. Riveiro, I. Maneiro, A. Barreiro, A. Monanno, G. Buscaino, A. Cuttitta, G. Basilone, S. Mazzola, 2008: *Estuarine Coastal and Shelf Science*. **77**, 775–78.
- Petruncio E.T., 1998: Observations of the Internal Tide in Monterey Canyon, *J. Geophys. Ocean.*, **28**, 1873–1903.
- Puig, P., A. Palanques, J. Guillen, and M. El Khatab, 2004: Role of internal waves in the generation of nepheloid layers on the northwestern Alboran slope: Implications for continental margin shaping, *J. Geophys. Res.*, **109**, 2156–2202.
- Reid, J.L., and Schwartzlose, R.A., 1962: Direct measurements of the Davidson Current off central California, *J. Geophys. Ocean.*, **6**, 2156–2202.
- Rines, J.E.B., P.L. Donaghay, M.M. Dekshenieks, J.M. Sullivan, and M.S. Twardowski, 2002: Thin layers and camouflage: hidden *Pseudo-nitzschia* spp. (Bacillariophyceae) populations in a fjord in the San Juan Islands, Washington. *Marine Ecology Progress Series*, **225**, 123–137.
- Rosenfeld, L.K., 1990: Baroclinic semidiurnal tidal currents over the continental shelf off northern California. *J. Geophys. Res.*, **95**, 2156–2202.
- Sandel, A.E., cited Jun 2009: 21st Century U.S. Navy Mine Warfare. [Available online at http://www.navy.mil/n85/miw_primer-june2009.pdf].
- SCRIPPS: Institution of Oceanography, cited 2013: Underwater Glider Spray. [Available online at <http://spray.ucsd.edu/pub/rel/index.php>]
- Stanton, T.P., and L.A. Ostrovsky, 1998: Observations of highly nonlinear internal solitons over the Continental Shelf. *J. Geophys. Res.*, **25**, 2695–2698.
- Yanez, Kathryn, 2012: The study of upper ocean stratification that controls the propagation of internal tidal bores in coastal areas M.S. thesis, Dept. of Undersea Warfare (Oceanography), Naval Postgraduate School.

THIS PAGE INTENTIONALLY LEFT BLANK

INITIAL DISTRIBUTION LIST

1. Defense Technical Information Center
Ft. Belvoir, Virginia
2. Dudley Knox Library
Naval Postgraduate School
Monterey, California